Low-Autocorrelation Binary Sequences: On Improved Merit Factors and Runtime Predictions to Achieve Them

Borko Bošković[a], Franc Brglez[b], Janez Brest[a]

[a]*Faculty of Electrical Engineering and Computer Science, University of Maribor, SI-2000 Maribor, Slovenia*
[b]*Computer Science, NC State University, Raleigh, NC 27695, USA*

Abstract

The search for binary sequences with a high figure of merit, known as the low autocorrelation binary sequence (`labs`) problem, represents a formidable computational challenge. To mitigate the computational constraints of the problem, we consider solvers that accept odd values of sequence length L and return solutions for skew-symmetric binary sequences only – with the consequence that not all best solutions under this constraint will be optimal for each L. In order to improve both, the search for best merit factor *and* the asymptotic runtime performance, we instrumented three stochastic solvers, the first two are state-of-the-art solvers that rely on variants of memetic and tabu search (`lssMAts` and `lssRRts`), the third solver (`lssOrel`) organizes the search as a sequence of independent contiguous self-avoiding walk segments. By adapting a rigorous statistical methodology to performance testing of all three combinatorial solvers, experiments show that the solver with the best asymptotic average-case performance, $\texttt{lssOrel\_8} = 0.000032 * 1.1504^L$, has the best chance of finding solutions that improve, as L increases, figures of merit reported to date. The same methodology can be applied to engineering new `labs` solvers that may return merit factors even closer to the conjectured asymptotic value of 12.3248.

Keywords: `Low-autocorrelation binary sequences`, `self-avoiding walk`, `stochastic combinatorial optimization`, `asymptotic average-case performance`

1. Introduction

The aperiodic low-autocorrelation binary sequence (`labs`) problem has a simple formulation: take a binary sequence of length L, $S = s_1 s_2 \ldots s_L$, $s_i \in \{+1, -1\}$, the autocorrelation function $C_k(S) = \sum_{i=1}^{L-k} s_i s_{i+k}$, and minimize the energy function:

$$E(S) = \sum_{k=1}^{L-1} C_k^2(S) \tag{1}$$

or alternatively, maximize the *merit factor* F [1, 2, 3]:

$$F(S) = \frac{L^2}{2E(S)}. \tag{2}$$

A binary sequence with the best merit factor has important applications in communication engineering. These sequences are used for example as modulation pulses in radar and sonar ranging [4, 5, 6]. To physicists, the optimum solution of the `labs` problem corresponds to the ground state of a generalized one dimensional Ising spin system with long range 4-spin interactions [7], also known as the Bernasconi model with aperiodic autocorrelation. The `labs` problem also appears in mathematics in terms of the Littlewood problem [8, 9], in chemistry [10], and in cryptography [11, 12]. Solving the `labs` problem is clearly important in a number of different areas. For more details, we refer the reader to surveys [13, 14].

The asymptotic value for the maximum merit factor F, introduced in [2], has been re-derived using arguments from statistical mechanics [7]:

$$\text{as} \quad L \to \infty, \quad \text{then} \quad F \to 12.3248 \tag{3}$$

The publication of the asymptotic value in Eq. 3 is providing an on-going challenge since no published solutions can yet claim to converge to this value as the length of the sequence increases.

Finding the optimum sequence is significantly harder than solving the special cases of the Ising spin-glass problems with limited interaction and periodic boundary conditions, for example [17]. While effective methods have been presented to solve the special cases up to $L = 400$ [17], the best merit factors that has also been *proven optimal* for the problem as formulated in Eq. 2 are presently known for values of $L \leq 60$ only [18]. A web page of `labs` best merit factors and solutions, up to the sequence length of $L = 304$, has been compiled by Joshua Knauer in 2002. This page is no longer accessible and has now been restored under [19] next to comprehensive tables of *best-value solutions*. These tables contain not only updates on the best known figures of merit but also the

Email addresses: `borko.boskovic@um.si` (Borko Bošković), `brglez@ncsu.edu` (Franc Brglez), `janez.brest@um.si` (Janez Brest)

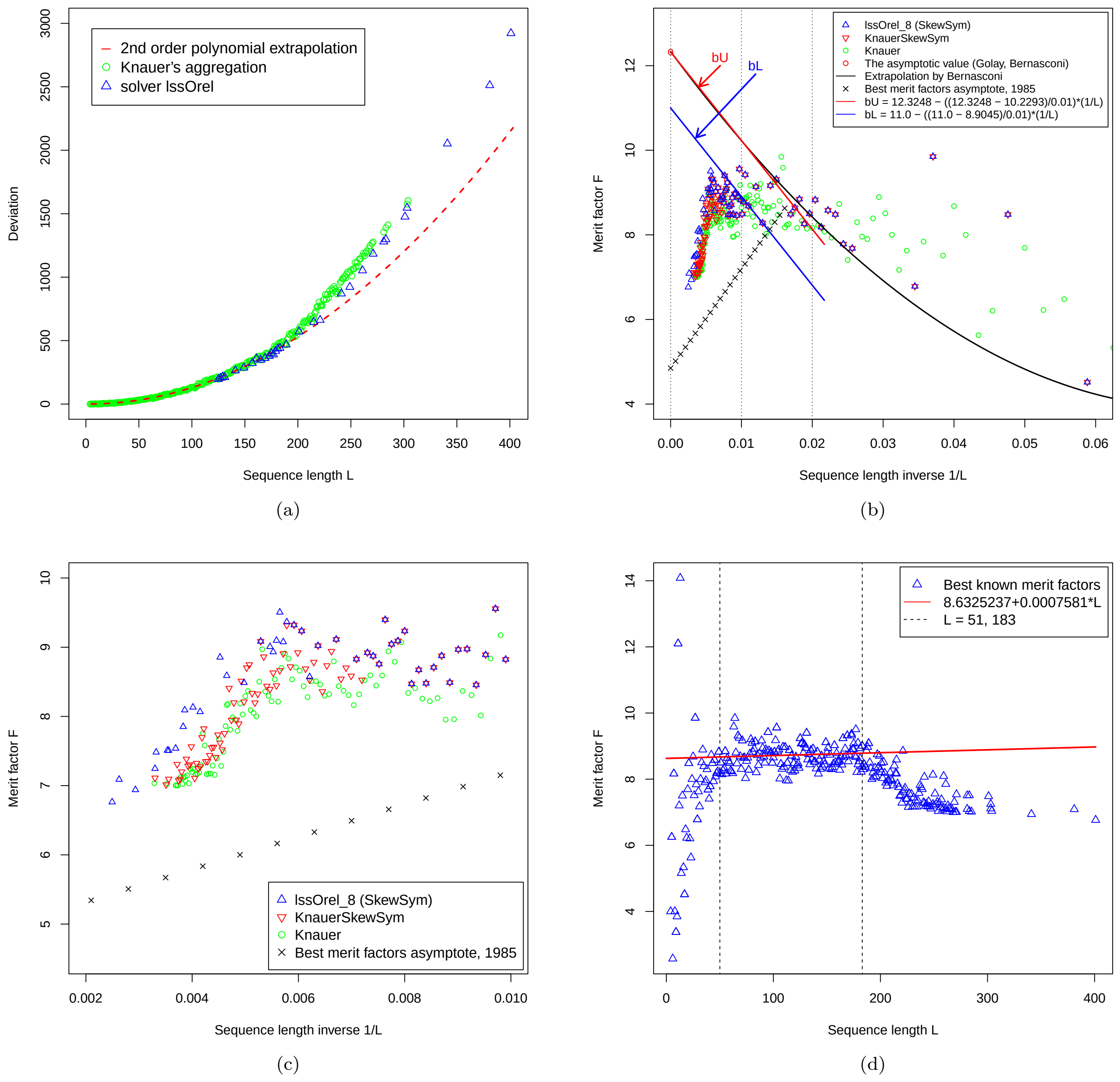

Figure 1: Asymptotic views of the **labs** problem best merit factors, aggregated from results with several generations of **labs** solvers: (a) A deviation-versus-length plot, introduced in [15], fits deviations from known optimal solutions for $L \le 60$ to a second-order polynomial (the dotted line); (b) A global view of the merit factor-versus-inverse sequence length, rigorously introduced in [7], demonstrates that the conjectured asymptotic value of $F = 12.3248$ may indeed be reachable with sufficient computational resources [2, 7], i.e. the improvements vis-a-vis the 'Best merit factors asymptote, 1985'[5] are significant [16]; (c) The expanded view of experimental results, particularly for $L > 183$ (or $1/L < 0.00546$) suggests that better merit factors may be found not only by providing massively parallel computational resources but also by continuing to improve the current generation of **labs** solvers; (d) A direct plot of merit factors F versus sequence length L illustrates that for $L \le 50$ there are large and also *asymmetrical* variations in values of merit factors, ranging from less than 4 to more than 14. For $L > 50$ and L $\le$ 183, i.e. for sequences where **lssOrel_8** solutions reports an *observed number of hits* larger than 1 (Figure 14), merit factor variations are not only significantly reduced, they also exhibit an *increasing trend* and lead to a linear predictor model $8.6325237 + 0.0007571 * L$. We demonstrate that, given the state-of-the-art **labs** solvers, the downwards trend in merit factors for $L > 183$ is due to insufficient application of computational resources – sequences with better merit values than the ones shown here exist and are expected to be found in the future!

number of *unique* solutions in *canonic form* and the solutions themselves. Relationships between results reported in [2, 5, 7, 3], and all subsequent updates under [19] are depicted in four panels in Figure 1. The latest experimental results support the trend towards the conjectured asymptotic value of $F = 12.3248$, however as we demonstrate later on in the paper, the computational cost to reach this value may well exceed the currently available resources unless a better solver is discovered.

While branch and bound solvers, for both even and odd sequences [18] and for skew-symmetric sequences only [20] have been pursued, they do not scale as well as the stochastic solvers. Stochastic solvers cannot prove optimality, they can only be compared on the basis of the *best-value solutions*, and to a limited extent, also on the average runtime needed to find such solutions under a sufficiently large number of repeated trials [21, 22, 23, 24, 25, 26, 27, 28, 29, 30]. The experimental results obtained with our stochastic solver `lssOrel` are compared to the instrumented versions of solvers in [30].[1]

Compared to heuristic methods, the body of the theoretical literature on the merit factor problem for binary sequences is considerable [14]. By 1983, it has been established by computation (R. J. Turyn) and made plausible by the ergodicity postulate, that long Legendre sequences offset by a quarter of their length have an asymptotic merit factor of 6 [31]. A rigorous proof for the asymptotic merit factor of 6, also based on the quarter-rotated Legendre sequences, has followed in 1991 [32]. The current records for asymptotic merit factors, obtained by *various construction techniques*, stand at 6.3421 [33, 34, 35, 36] and 6.4382 [37]. Clearly, the challenge of finding long binary sequences that would converge towards the asymptotic merit factor of $F = 12.3248$, as postulated in Eq. 3, remains open for experimentalists as well as for theoreticians.

The paper is organized as follows. Section 2 introduces notation, definitions, and examples that motivate the approach taken in this paper. Section 3 highlights details about three `labs` solvers as they are instrumented for comparative performance experiments to measure, in a platform-independent manner, solver's asymptotic performance as the size of the `labs` problem increases. Section 4 summarizes results of extensive experiments with these solvers, including bounds and projections for computational resources needed to increase the likelihood of finding better solutions of the `labs` problem for sizes $L > 141$. The section concludes with two views of merit factors as L increases towards the value of 5000. The first view depicts an asymptotic convergence of merit factor towards 6.34, achievable by constructing each sequence under runtime polynominal complexity of $O(L^3)$. The second view outlines challenges for the next generation of labs solvers. Given current computational resources, the trend of merit factors achieved with `lssOrel_8` points in the right direction; however, sequences that would converge closer to the conjectured asymptotic value of 12.3248 are yet to be discovered and will be the focus of future work.

2. Notation and Definitions

This section follows notation, definitions, and metaphors introduced in [38] and [39]. The first paper defines Hasse graphs and relates them to average-case performance of combinatorial optimization algorithms, the second paper demonstrates merits of *long and entirely contiguous self-avoiding walks* which are searching, under concatenation of binary and ternary coordinates, for the maximum number of bonds in the 2D protein folding problem. Combined, these papers also support a simple and intuitive introduction of the *self-avoiding walk segments* as the key component of an effective strategy which we apply to finding best solution to instances of the `labs` problem in this paper. There are two illustrations of such walks: a small one in Figure 2 at the end of this section, and a larger instance in Section 3 where, in Figure 5, we compare a self-avoiding walk induced by our solver `lssOrel` with a walk based on tabu search induced by the solver `lssMAts` [30]. We proceed with a brief reprise of notation and definitions, some of them extended to specifics of the `labs` problem.

Solution as a coordinate-value pair. While the energy of the autocorrelation function as defined in Eq. 1 may be simple to interpret in terms of binary symbols $s_i \in \{+1, -1\}$, we define, for the remainder of the paper, any solution of Eq. 1 as a coordinate-value pair in the form

$$\underline{\varsigma} : \Theta(\underline{\varsigma}) \tag{4}$$

where $\underline{\varsigma}$ is a binary string of length L, also denoted as the *coordinate* from $[0,1]^L$, and $\Theta(\underline{\varsigma})$ is the *value* associated with this coordinate (an integer value denoting energy as shown in Eq. 1).

Coordinate distance. The distance between two binary coordinates $\underline{a}$ and $\underline{b}$ is defined as the Hamming distance:

$$d(\underline{a}, \underline{b}) = \sum_{i=1}^{L} a_i \oplus b_i \tag{5}$$

Coordinate symmetries. There are four coordinate transformations that reveal the symmetries of the `labs` problem function as formulated in Eq. 1:

complementation: For example, the complement of 0000011001010 is 1111100110101

reversal: For example, the reversal of 0000011001010 is 0101001100000

symmetry: For example, for L even, we say that 011110 is symmetric compared to $L/2$ without coordinate complementation.

skew-symmetry: Skew-symmetry has been introduced in [1]. It is defined for odd values of L only and the solution of the `labs` problem can be expressed with coordinates that are significantly reduced in size:

$$L' = (L+1)/2$$

For example, 0000011001010 is skew-symmetric since $(L-1)/2$ left-most coordinates and $(L-1)/2$

[1]The generosity of authors to provide the source code of `lMAts`, `lssMAts` and its derivative, `lssRRts`, is greatly appreciated. The robust performance of these solvers has revealed additional insights about the `labs` problem.

right-most coordinates are skew-symmetric under coordinate reversal. Formally, the skew-symmetry definition in terms of binary coordinate components b_k and their complements $\overline{b}_k$ is

$$b_{L'+i} = \begin{cases} \overline{b}_{L'-i} & \text{if } i = 1, 3, 5, ... \\ b_{L'-i} & \text{if } i = 2, 4, 6, ... \end{cases} \tag{6}$$

The introduction of skew-symmetry significantly reduces the computational complexity of the `labs` problem – but not every optimal solution for odd values of L is also skew-symmetric. Only recently, a branch-and-bound solver [12, 20] extended known optimal solutions for skew-symmetric sequences to length up to 119. However, even under skew-symmetry, only stochastic solvers have demonstrated the potential to find improved, if not optimal solutions, as L increases to 201 and beyond.

Canonic solutions and best upper bounds. The `labs` problem symmetries partition solutions into four quadrants with coordinate prefixes of `00`, `01`, `10`, and `11`. Without loss of generality, we transform coordinates of all optimal or *best value* solutions found in quadrants `01`, `10`, `11` to the quadrant `00` and denote the set of unique optimal `coordinate:value` solution pairs in the quadrant `00` as the *canonic solutions set*. For a given L, only the coordinates in this set are unique; the optimum or the best known value, also denoted as *the best upper bound* Θ_L^{ub} is the same for each coordinate in this set. We say that C_L is the cardinality of canonic solutions set and that Θ_L^{ub} is the best upper bound we associate with the `labs` instance of size L.

Distance=1 neighborhood. The distance=1 neighborhood of a coordinate $\underline{\varsigma}_j$ is a set of coordinates

$$\mathcal{N}(\underline{\varsigma}_j) = \{ \ \underline{\varsigma}_j^i \mid d(\underline{\varsigma}_j, \underline{\varsigma}_j^i) = 1, \quad i = 1, 2, \ldots, L \ \} \tag{7}$$

Informally, a binary coordinate $\underline{\varsigma}_j$ of size L, also called a *pivot coordinate*, has L neighbors, each a distance of 1 from the pivot coordinate.

Contiguous walks and pivot coordinates. Let the coordinate $\underline{\varsigma}_0$ be the initial coordinate from which the walk takes the first step. Then the sequence

$$\{\underline{\varsigma}_0, \underline{\varsigma}_1, \underline{\varsigma}_2, \ldots, \underline{\varsigma}_j, \ldots, \underline{\varsigma}_\omega\} \tag{8}$$

is called a *walk list* or a *walk* of length ω, the coordinates $\underline{\varsigma}_j$ are denoted as *pivot coordinates* and $\Theta(\underline{\varsigma}_j)$ are denoted as *pivot values*. Given an instance of size L and its best upper bound Θ_L^{ub}, we say that the walk *reaches* its target value (and stops) when $\Theta(\underline{\varsigma}_\omega) \le \Theta_L^{ub}$.

We say that the walk is contiguous if the distance between adjacent pivots is 1; i.e., given Eq. 5, we find

$$d(\underline{\varsigma}_j, \underline{\varsigma}_{j-1}) = 1, \quad j = 1, 2, ..., \omega \tag{9}$$

Self-avoiding walks (SAWs). We say that the walk is *self-avoiding* if all pivots in Eq. 8 are unique. We say that the walk is composed of two or more *walk segments* if the initial pivot of each walk segment has been induced by a well-defined heuristic such as *random restarts*, a heuristic associated also with all solvers described in this paper. Walk segments can be of different lengths and if viewed independently of other walks, may be self-avoiding or not. A walk composed of two or more self-avoiding walk segments may no longer be a self-avoiding walk, since some of the pivots may overlap and also form cycles. This is illustrated after we define the Hasse graph below.

Hasse graph. Hasse graph has been defined in [38, 39] as a model of hyperhedron (or informally, a dice) based on an extension of the Hasse diagram. In the case of the `labs` problem, Hasse graph is an undirected *labeled graph* with 2^L vertices and $L \times 2^{L-1}$ edges; the degree of each vertex is L and the label is the pair $\underline{\varsigma} : \Theta(\underline{\varsigma})$ as defined in Eq. 4. By projecting this graph with its labeled vertices onto a plane, we can not only illustrate concepts of coordinate/pivot neighborhoods but also specific walks as a combinatorial search heuristics.

Figure 2 illustrates not only two Hasse graphs, with each vertex displaying a *coordinate:value*; it also illustrates that the target value can be reached either by a sequence of three shorter SAW segments (each segment represents a contiguous SAW) or by a single contiguous SAW. The three contiguous *self-avoiding walk segments* in Figure 2a have lengths of 7, 7, and 4, covering a total of 19 vertices in 18+2=20 steps. We add two steps since the second and the third walk segment are induced by two restarts. Just as the pivot $\underline{\varsigma}_0$ is the initial pivot for the first step in the first walk, pivots $\underline{\varsigma}_7$ and $\underline{\varsigma}_{15}$ are taken as initial pivots for the first step in the second walk and the first step in the third walk, respectively. Here is a linear depiction of the 19 vertices and three walk segments.

$$\bullet\underbrace{\bullet\bullet\bullet\bullet\bullet\bullet\bullet\bullet}_{7} \quad \underbrace{\bullet\bullet\bullet\bullet\bullet\bullet\bullet}_{7} \quad \underbrace{\bullet\bullet\bullet\bullet}_{4}$$

To keep the Hasse graph less cluttered, the steps of the walk that are induced by two restarts are not shown with additional edges. We denote such steps as *jump steps* since the distance between pivots may exceed 1. For example, $d(\underline{\varsigma}_8, \underline{\varsigma}_7) = d(\texttt{10100}, \texttt{01111}) = 4$ and $d(\underline{\varsigma}_{16}, \underline{\varsigma}_{15}) = d(\texttt{11010}, \texttt{11011}) = 1$.

A more formal description of SAW as a general purpose combinatorial search algorithm is given in Section 3. A summary of results in Section 4 demonstrates that in the asymptotic sense (as L increases), a contiguous SAW has walk lengths that are on the average shorter than walk lengths achieved under heuristic which limits the length of each SAW and then, with repeated random restarts, assembles the shorter SAWs into a single long walk. In general, the assembled walk is no longer contiguous, see Figure 2a.

On origins of self-avoiding walks. The notion of self-avoiding walks (SAWs) was first introduced by the chemist Paul Flory in order to model the real-life behavior of

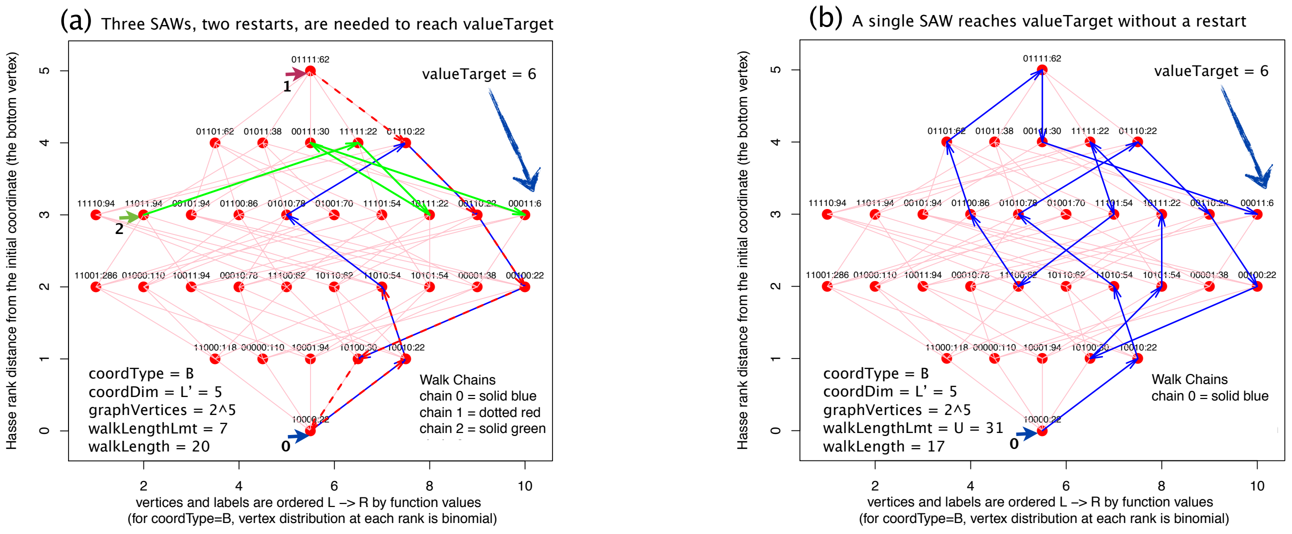

(a) Three SAWs, two restarts, are needed to reach valueTarget
valueTarget = 6
coordType = B
coordDim = L' = 5
graphVertices = 2^5
walkLengthLmt = 7
walkLength = 20
Walk Chains
chain 0 = solid blue
chain 1 = dotted red
chain 2 = solid green
(b) A single SAW reaches valueTarget without a restart
valueTarget = 6
coordType = B
coordDim = L' = 5
graphVertices = 2^5
walkLengthLmt = U = 31
walkLength = 17
Walk Chains
chain 0 = solid blue
Hasse rank distance from the initial coordinate (the bottom vertex)
vertices and labels are ordered L –> R by function values
(for coordType=B, vertex distribution at each rank is binomial)

Figure 2: Two cases of self-avoiding walks (SAWs): (a) three SAWs where each SAW is limited to 7 or less steps and is followed by random restarts; (b) a single SAW where the number of steps is limited by the total number of vertices in the graph. In general, the average walk length required to reach the target value from any starting point will be less when the walk is self-avoiding and contiguous rather than when the walk is composed from multiple shorter self-avoiding walk segments. Nominally, this is an instance of size $L = 13$; here we are solving the instance under skew-symmetry, so $L' = 7$. By considering the canonical solutions only (i.e. solutions with the coordinate prefix of 00), we can use a Hasse graph with only $2^5 = 32$ vertices to illustrate such walks.

chain-like entities such as solvents and polymers, whose physical volume prohibits multiple occupation of the same spatial point [40]. In mathematics, a SAW lives in the n-dimensional lattice $\mathbb{Z}^n$ which consists of the points in $\mathbb{R}^n$ whose components are all integers [41, 42]. The challenge of finding the longest self-avoiding walk in multi-dimensional lattices *efficiently* has been and also continues to be of considerable interest in physics [43].

3. Solver Instrumentation and Solvers

We have instrumented a total of four solvers to conduct the experiments summarized in the follow-up sections. Solvers `lMAts` and `lssMAts`, described in [30], implement a memetic-tabu search strategy. The solver `lMAts` returns solutions for both even and odd sequences, the solver `lssMAts` returns skew-symmetric sequences only. The solver `lssRRts`, is a special case of `lssMAts`. Our solver, `lssOrel`, implements a self-avoiding walk strategy for odd sequences under skew-symmetry so that experimental results with `lssOrel` can be directly compared with `lssMAts` and `lssRRts`.

We begin with *solver instrumentation*, follow up with solver pseudo-code descriptions, and conclude with highlights on differences between `lssMAts` and `lssOrel`.

Solver instrumentation. We argue that in order to design a better combinatorial solver one also needs to devise an environment and a methodology that supports reproducible and statistically significant computational experiments. In our case, this environment continues to evolve under the working name of `xBed` [44]. A generic and standardized notation is an important part of this environment; Table 1 summarizes the notation and description of principal variables in our solver instrumentation which we also use in our pseudo-code descriptions.

For example, reporting the *runtime* or t is not the only performance variable of importance. The most important variable is the variable named as *cntProbe* or τ: a variable that counts how many times the solver evaluates the objective function before completing the run. By keeping track of this variable, we can compare two solvers regardless of the platform on which experiments have been performed, and regardless whether the solver represents a much slower scripted implementation of an early prototype or the faster compiled-code implementation. In our experiments, the correlation coefficient between *runtime* and *cntProbe* consistently exceeds 0.999.

Given the labs problem of size L, the experiment is defined by N runs of the solver where each run is considered a sequence of *Bernoulli trials* which are probing the objective function: the solver stops as soon as – and only when – it finds the coordinate $\underline{\varsigma}^*$ with the best known solution value $\Theta(\underline{\varsigma}^*) = \Theta_L^{ub}$. If the solver does not time-out, the status variables recorded with each run are *targetReached* $= 1$ and *isCensored* $= 0$ or *targetReached* $= 2$ and *isCensored* $= 0$. If the solver returns a solution $\Theta(\underline{\varsigma}^*) < \Theta_L^{ub}$, we record *targetReached* $= 2$, declare $\Theta_L^{ub} = \Theta(\underline{\varsigma}^*)$ as the new best known solution value, and initiate a new series of Bernoulli trials with the new value of Θ_L^{ub}. If the solver terminates the run before reaching the target value Θ_L^{ub} (due to a time-out limit), we record *targetReached* $= 0$ and *isCensored* $= 1$. Each time *targetReached* $= 1$ is recorded, the counter that measures the *observed number of hits*,

Table 1: Summary of notation: symbols, names, and descriptions.

symbol	**short name**	**brief description**
L	coordDim	instance size
L'	coordDim'	instance size under skew-symmetry $(L+1)/2$
σ_0	seedInit	initial seed integer
$\underline{\varsigma}_0$	coordInit	initial coordinate
$\Theta(\underline{\varsigma}_0)$	valueInit	initial value
$\underline{\varsigma}_j$	coordPivot	pivot coordinate
$\Theta(\underline{\varsigma}_j)$	valuePivot	pivot value
$\underline{\varsigma}_j^i$	coordNeighb	pivot neighbor coord.
$\mathcal{N}(\underline{\varsigma}_j)$	coordNeighbSet	full neighborhood set of pivot coordinate
$\mathcal{N}_{saw}(\underline{\varsigma}_j)$	sawNeighbSet	SAW neighborhood set
ω_c	walkSegmCoef	walk segment coefficient
$\omega_{lmt} = \omega_c \times L'$	walkSegmLmt	walk segm. length limit
$Walk_\omega = \{\underline{\varsigma}_0, \ldots, \underline{\varsigma}_\omega\}$	walkList	walk list after ω steps
t	runtime	CPU runtime
t_{lmt}	runtimeLmt	solver timeout value
τ	cntProbe	# of function probes
ρ	cntRestart	# of walk restarts

For `labs` problems with an odd value of L, $L' = (L+1)/2$ represents a *de facto* instance size under skew-symmetry.

symbol	**short name**	**brief description**
β	cntTrapped	# of trapped solutions
$\underline{\varsigma}^*$	coordBest	best coordinate
$\Theta(\underline{\varsigma}^*)$	valueBest	best value
Θ_L^{ub}	valueTarget	best upper bound
	targetReached	solution status: 0 if $\Theta(\underline{\varsigma}^*) > \Theta_L^{ub}$, 1 if $\Theta(\underline{\varsigma}^*) = \Theta_L^{ub}$, 2 if $\Theta(\underline{\varsigma}^*) < \Theta_L^{ub}$
	isCensored	solution censure status: 1 if $t \geq t_{lmt}$ (targetReached = 0); 0 otherwise (targetReached = 1 or 2)
N	sampleSize	# of instances and initial seeds in the experiment
N_c	sampleSizeCrit	$N_c \geq 100$ to satisfy $CI_{0.95} \approx [0.8 \times \overline{m},\ 1.2 \times \overline{m}]$
$\overline{m}$	sampleMean	an estimate of the sample mean
$hitO$	hitsObserved	# of observed uncensored solutions (hits)
$hitO_r$	hitRatioObserved	observed hit ratio, $hitO/N$
$hitP$	hitsPredicted	# of predicted uncensored solutions (hits)
$hitP_r$	hitRatioPredicted	predicted hit ratio, $hitP/N$
$solvP$	solvPredicted	predicted solvability or waiting time for a single solver
$solvP_{ser}$	solvPredictedSer	predicted solvability or waiting time for N serial solvers

For `labs` problems, $\Theta(\underline{\varsigma}^*)$ represents the *minimum energy value* returned by the solver.

hitO, is incremented:

$$hitO \overset{\text{def}}{=} \text{number of successes or } hits \text{ in } N \text{ runs.} \quad (10)$$

Concurrently with the observed number of hits *hitO*, we also define the *observed hit ratio*, $hitO_r$:

$$hitO_r \overset{\text{def}}{=} hitO/N \quad (11)$$

The *sampleSize* of the experiment is thus N: the experiment is performed either serially on a single processor or in parallel on a grid of N processors.

Given the probability of success on any *single* Bernoulli trial as p, then the number of probes T required to obtain the first success has geometric distribution with parameter p. Formally, the probability of observing the first success on τ-th probe or before is thus

$$P(T = \tau) = (1-p)^{\tau-1}p \quad (12)$$

The cumulative distribution function $F_T(\tau)$ is then

$$P(T \leq \tau) = F_T(\tau) = 1 - (1-p)^\tau \quad (13)$$

i.e. the probability that the solver finds the solution before or on probe τ is the cumulative probability $F_T(\tau)$. Experimentally, the time required until a success occurs is proportional to the number of probes, hence T also denotes the *waiting time*, a characteristic value associated with the solver.

Traditionally, the waiting time is considered as a continuous random variable and for $p < 0.01$ we can approximate, with negligible error, the distribution function $F_T(\tau)$ with a cumulative exponential distribution function

$$P(T < \tau) = F_T(\tau) = 1 - exp(-\tau/\overline{m}) \quad (14)$$

where $\overline{m} = 1/p$. Given the sample size N, we estimate the value of p either by computing the mean value of $\overline{m}$ either as *cntProbe* τ or *runtime* t in units of seconds, minutes, hours, days, etc. In other words, given a solver with an estimated value of $\overline{m} = 10$ hours, the probability that this solver returns the target solution value in 10 hours (or less) is 0.632: by waiting for 20, 40, or 80 hours, the probability of a *hit* increases to 0.865, 0.982, or 0.999, respectively.

The performance experiments summarized in the next section confirm that the *uncensored* random variables such as *runtime* or *cntProbe* have near-exponential or near-geometric distribution, i.e. we observe $s \approx \overline{m}$ where s denotes the sample standard deviation and $\overline{m}$ denotes the sample mean. Under such distributions, given the uncensored sample size of $N_c = 100$ used in all of our experiments, a reliable rule-of-thumb estimate of the 95% confidence interval ($CI_{0.95}$) on value of the sample mean $\overline{m}$ is thus

$$CI_{0.95} \approx [0.8 \times \overline{m},\ 1.2 \times \overline{m}] \text{ ... uncensored } N_c = 100 \quad (15)$$

When a subset of N_c runs is censured, the confidence interval can increase significantly beyond the one in Eq. 15. We argue that reliable estimates of confidence bounds on the mean values of *runtime* or *cntProbe* returned by combinatorial solvers under censoring are a subject best left to statisticians [45].

The question now arises whether and how, for a given solver and a labs instance, we can *predict* the number of hits, *hitP*, as well as the hit ratio, $hitP_r$. The answer can be formulated in the context of the solver time-out value or runtime limit t_{lmt}:

$$hitP_r \stackrel{\text{def}}{=} 1 - exp(-t_{lmt}/\overline{m}) \tag{16}$$

Thus, the predicted hit ratio $hitP_r$ in Eq. 16 is just an instance of the cumulative exponential distribution function in Eq. 14. When the experiment is performed serially on a single processor, we assume that the solver is the only significant application scheduled to run on the processor, so the value of t_{lmt} represent the true runtime limit. However, when the experiment is performed in parallel on a grid of N processors, each processor is scheduled to run a number of applications and the value of t_{lmt} is reduced by a $loadFactor > 1$, a random variable with an empirical average value of 2.4 for our environment under [46].

Similarly, we define and calculate the *predicted the number of hits, hitP*:

$$hitP \stackrel{\text{def}}{=} \lfloor N \times hitP_r \rfloor \tag{17}$$

In Section 4, we empirically derive the runtime model for the solver `lssOrel` to predict a runtime mean. Consider a labs instance for $L = 149$. The model predicts a runtime mean of $0.000032 * 1.1504^{149}/(3600) = 10.34928$ hours. For a runtime limit $t_{lmt} = 96$ hours (4 days) and $N = 100$ processors, Eqs. 16 and 17 predict $hitP_r = 0.9999055$ and $hitP = 99$ – under the assumption of $loadFactor = 1$. Under the empirically verified value of $loadFactor = 2.4$ under [46], our predictions are modified to $hitP_r = 0.9789588$ and $hitP = 97$. The experiments on the grid, summarized in Figure 15 illustrate that for $L = 149$ the solver `lssOrel` reports the *observed hit ratio* $hitO = 95$.

Given that $hitO = 95 < N_c$ with $N_c = 100$ as postulated in Eq. 15, the question arises how many processors N should be scheduled on the grid, so that for each value of L, we can maintain $hitO \geq N_c = 100$ with the runtime limit of $t_{lmt} = 96$ hours? A quick back-of-the envelope calculation returns the answer for $L = 149$: $N = 103$. More formally, we find the answer as follows:

$$N \stackrel{\text{def}}{=} \lceil N_c/hitP_r \rceil \tag{18}$$

Two more examples for the runtime limit of $t_{lmt} = 96$, extrapolated from Figure 15: (1) for $L = 165$ we find $hitP_r = 0.3365782$ and $N = 298$ in order to achieve $N_c = 100$ hits, and (2) for $L = 179$ we find $hitP_r = 0.05607801$ and $N = 1784$ in order to achieve $N_c = 100$ hits.

An experiment of a sample size N performed in parallel with N solvers on a grid of N processors has a significant advantage in terms of "waiting time" when compared to an experiment where the solver is invoked N times on a single processor. However, serially scheduled experiments are important in this research: they support not only accurate runtime comparisons of different solvers but also allow accurate observations of statistically significant differences, if any, between two or more heuristics implemented by the same solver. Consider again the labs instance for $L = 149$ analyzed after Eq. 17: the value of the runtime mean is 10.34928 hours and when invoking the solvers in parallel on $N = 100$ processors we predict to reach the hit ratio $hitP_r > 0.99$ in 96 hours (4 days). When invoking the solver N times on a single processor, the sum of the exponential variates returned by each run has *gamma distribution*. For relationships between Poisson's processes, exponential distributions, and gamma distributions, see [47].

Using the notation of R [48], the cumulative gamma function *pgamma* and its inverse *qgamma*:

$$P(T \leq t_{lmt}) = hitP_{ser} \stackrel{\text{def}}{=} pgamma(t_{lmt}, N, 1/\overline{m}) \tag{19}$$

In queueing theory, we associate the inverse of the cumulative gamma function *qgamma* with the *waiting time*. In this paper, given $hitP_{ser}$ as the solver's predicted hit rate of N solvers invoked serially, the inverse of cumulative gamma function is the metaphor for the *predicted solvability* $solvP_{ser}$ of N serially invoked solvers:

$$solvP_{ser} \stackrel{\text{def}}{=} qgamma(hitP_{ser}, N, 1/\overline{m}) \tag{20}$$

Using Eq. 20 (the inverse of Eq. 19), we can compute the solvability $solvP_{ser}$ directly. Given a solver with $\overline{m} = 10.34928$ and the hit rate of 99/100, we use *qgamma* and find $qgamma(0.99, 100, 10.34928) = 1290.79$ hours (53.8 days).

In the case of the single solver with predicted hit ratio $hitP_r$, we again use *qgamma* to compute the *predicted solvability solvP* of this single solver:

$$solvP \stackrel{\text{def}}{=} qgamma(hitP_r, 1, 1/\overline{m}) \tag{21}$$

Table 2 presents values of cumulative gamma function in the range of most practical interest for our purposes. Note that for $N = 100$, $pgamma(125, 100, 1) = 0.9906$ and that for $N = 1$, $pgamma(q, 1, 1)$ is equivalent to the cumulative distribution of the exponential function.

Table 2: A detail about pg(q, r) = pgamma(q, r, 1) in R.

q	pg(q, 1)	pg(q, 2)	pg(q, 4)	q	pg(q, 100)
1	0.6321	0.2642	0.0189	80	0.0171
2	0.8647	0.5939	0.1428	90	0.1582
3	0.9502	0.8009	0.3528	100	0.5133
4	0.9817	0.9084	0.5665	110	0.8417
5	0.9933	0.9596	0.7349	120	0.9721
8	0.9997	0.9969	0.9576	125	0.9906
10	0.9999	0.9995	0.9897	135	0.9993

Solver `lssOrel`. A self-avoiding walk strategy implemented by `lssOrel` follows a few simple rules: (1) initialize a coordinate $\underline{\varsigma}$ and mark it as the 'initial pivot'; (2) probe all unmarked adjacent coordinates, then select and mark the coordinate with the 'best value' as the new pivot. In the case when more than one adjacent coordinates have best value, one of them is randomly selected as a new pivot; (3) continue the walk until either $\Theta(\underline{\varsigma}^*) \leq \Theta_L^{ub}$ or the walk is blocked by adjacent coordinates that are already pivots;

```
procedure lssOrel($\sigma_0, \Theta_L^{ub}, t_{lmt}, \omega_{lmt}$)
    $\underline{\varsigma}_0 : \Theta(\underline{\varsigma}_0) \leftarrow$ coordInit($\sigma_0$)                ▷ initial solution
    $\tau \leftarrow 1$                                            ▷ initialize cntProbe
    $\underline{\varsigma}^* : \Theta(\underline{\varsigma}^*) \leftarrow \underline{\varsigma}_0 : \Theta(\underline{\varsigma}_0)$            ▷ initial best solution
    $isCens \leftarrow 0$                                          ▷ initialize $isCensored$
    $tgReached \leftarrow 0$                                       ▷ initialize $targetReached$
    $\beta \leftarrow 0$                                            ▷ initialize $cntTrapped$
    $\omega \leftarrow 0$                                           ▷ initialize total number of steps
    while true do
        $\omega_s : \underline{\varsigma}^* : \Theta(\underline{\varsigma}^*) \leftarrow$ walk.saw($\underline{\varsigma}_0 : \Theta(\underline{\varsigma}_0), t_{lmt}, \omega_{lmt}$)   ▷ return a completed walk segment
        $\omega \leftarrow \omega + \omega_s$                            ▷ update total number of steps
        if $\Theta(\underline{\varsigma}^*) \leq \Theta_L^{ub}$ then
            if $\Theta(\underline{\varsigma}^*) = \Theta_L^{ub}$ then
                $tgReached = 1$                                ▷ upper-bound is reached
            else
                $tgReached = 2$                                ▷ upper-bound is improved
            end if
            break
        end if
        if $t \geq t_{lmt}$ then
            $isCens \leftarrow 1$                                 ▷ return solution as "censored"
            break
        end if
        $\underline{\varsigma}_0 : \Theta(\underline{\varsigma}_0) \leftarrow$ coordInit()               ▷ initialize a new walk segment
        $\tau \leftarrow \tau + 1$                                     ▷ update $cntProbe$
        $\omega \leftarrow \omega + 1$                                     ▷ update total number of steps
    end while
    $Table \leftarrow (\sigma_0, \underline{\varsigma}^*, \Theta(\underline{\varsigma}^*), \omega, \tau, t, isCens, tgReached)$
end procedure
```

```
procedure walk.saw($\underline{\varsigma}_0 : \Theta(\underline{\varsigma}_0), t_{lmt}, \omega_{lmt}$)
    if $\Theta(\underline{\varsigma}_0) \leq \Theta(\underline{\varsigma}^*)$ then
        $\underline{\varsigma}^* : \Theta(\underline{\varsigma}^*) \leftarrow \underline{\varsigma}_0 : \Theta(\underline{\varsigma}_0)$      ▷ new best solution
    end if
    $\omega_s \leftarrow 0$                                  ▷ walk segment length
    $Walk_0 \leftarrow \{\underline{\varsigma}_0\}$                            ▷ new walk segment
    while $\Theta(\underline{\varsigma}^*) > \Theta_L^{ub}$ and $\omega_s < \omega_{lmt}$ do
        if $t \geq t_{lmt}$ then                         ▷ timeout
            break
        end if
        $\omega_s = \omega_s + 1$                           ▷ a new step!
        $Walk_{\omega_s} : \underline{\varsigma}_{\omega_s} : \Theta(\underline{\varsigma}_{\omega_s}) \leftarrow$
            $\leftarrow$ newPivot.saw($\underline{\varsigma}_{\omega_s - 1}, Walk_{\omega_s - 1}$)
        if $\Theta(\underline{\varsigma}_{\omega_s}) \leq \Theta(\underline{\varsigma}^*)$ then
            $\underline{\varsigma}^* : \Theta(\underline{\varsigma}^*) \leftarrow \underline{\varsigma}_{\omega_s} : \Theta(\underline{\varsigma}_{\omega_s})$
        end if
    end while
    return $\omega_s : \underline{\varsigma}^* : \Theta(\underline{\varsigma}^*)$
end procedure
```

```
procedure newPivot.saw($\underline{\varsigma}_{\omega_s - 1}, Walk_{\omega_s - 1}$)
    $\mathbb{Z} \leftarrow i = 1, 2, \ldots, L$
    $\mathbb{Z}_p \leftarrow permute(\mathbb{Z})$
    $\mathcal{N}(\underline{\varsigma}_{\omega_s - 1}) \leftarrow \{\underline{\varsigma}^i_{\omega_s - 1} | d(\underline{\varsigma}_{\omega_s - 1}, \underline{\varsigma}^i_{\omega_s - 1}) = 1, i \in \mathbb{Z}_p\}$
    $\mathcal{N}_{saw}(\underline{\varsigma}_{\omega_s - 1}) \leftarrow \{\mathcal{N}(\underline{\varsigma}_{\omega - 1}) | \underline{\varsigma}^i_{\omega_s - 1} \notin Walk_{\omega_s - 1}\}$
    if $\mathcal{N}_{saw}(\underline{\varsigma}_{\omega_s - 1}) \neq \emptyset$ then
        $\underline{\varsigma}_{\omega_s} : \Theta(\underline{\varsigma}_{\omega_s}) \leftarrow$ bestNeighbor($\mathcal{N}_{saw}(\underline{\varsigma}_{\omega_s - 1})$)
        $Walk_{\omega_s} \leftarrow Walk_{\omega_s - 1} \cup \{\underline{\varsigma}_{\omega_s}\}$
        $\tau \leftarrow \tau + | \mathcal{N}_{saw}(\underline{\varsigma}_{\omega_s - 1}) |$          ▷ update $cntProbe$
    else                                   ▷ deal with a trapped pivot
        $\beta = \beta + 1$
        $\underline{\varsigma}_{\omega_s} : \Theta(\underline{\varsigma}_{\omega_s}) \leftarrow$ coordInit()                ▷ re-initialize
        $Walk_{\omega_s} \leftarrow \{\underline{\varsigma}_{\omega_s}\}$
        $\tau \leftarrow \tau + 1$                              ▷ update $cntProbe$
    end if
    return $Walk_{\omega_s} : \underline{\varsigma}_{\omega_s} : \Theta(\underline{\varsigma}_{\omega_s})$
end procedure
```

Figure 3: A fully instrumented version of solver lssOrel and two supporting procedures: walk.saw and newPivot.saw. Procedure lssOrel: as a single contiguous self-avoiding walk or as a sequence of contiguous self-avoiding walk segments. Procedure walk.saw: Self-avoiding walk with a sequence of best pivot coordinates. Procedure newPivot.saw: Searching for the best new pivot under restrictions of SAW.

(4) if the walk is blocked or its length exceeds a threshold, initialize a new coordinate $\underline{\varsigma}^i$ as a 'new initial pivot' and restart a new walk segment; (5) manage the memory constraints with an efficient data structure such as a hash table. For examples of contiguous and non-contiguous self-avoiding walks, see Figure 2.

In Figure 3 we present the fully instrumented pseudo code of solver lssOrel. The main procedure lssOrel invokes walk.saw which in turn invokes newPivot.saw. Depending on initial parameters, the procedure lssOrel returns the best solution from a single contiguous self-avoiding walk or a sequence of contiguous self-avoiding

```
1:  procedure lssMAts($\Theta_L^{ub}$, $t_{lmt}$)
2:    for $i \leftarrow 1$ to $popsize$ do
3:      $pop_i \leftarrow$ RandomBinarySequence($L$)
4:      Evaluate($pop_i$)
5:    end for
6:    $\Theta(\varsigma^*) \leftarrow$ ValueBest(pop)
7:    while $t < t_{lmt}$ and $\Theta(\varsigma^*) > \Theta_L^{ub}$ do
8:      for $i = 1$ to $offsize$ do
9:        if recombination is performed ($p_X$) then
10:         $parent_1 \leftarrow$Select($pop$)
11:         $parent_2 \leftarrow$Select($pop$)
12:         $offspring_i \leftarrow$Recombine($parent_1, parent_2$)
13:       else
14:         $offspring_i \leftarrow$Select($pop$)
15:       end if
16:       if mutation is performed ($p_m$) then
17:         $offspring_i \leftarrow$Mutate($offspring_i$)
18:       end if
19:       $offspring_i \leftarrow$TabuSearch($offspring_i$)
20:       Evaluate($offspring_i$)
21:     end for
22:     $pop \leftarrow$Replace($pop$, $offspring$)
23:     $\Theta(\varsigma^*) \leftarrow$ ValueBest(pop)
24:   end while
25: end procedure
```

(a) lssMAts solver, based on MA_{TS} in [30].

The procedure lssMAts on the left is an instrumented versions of the labs solver named as MA_{TS} in [30]. Settings of all parameters, used also in our experiments, are described in [30]. See a concise reprise below.

setting	value
population size:	100
mutation probability:	$2/(L+1)$
crossover probability:	0.9
tournament selection size:	2
crossover:	uniform
tabu search walk length:	a random choice from the range $[\frac{L}{2}, \frac{3L}{2}]$

```
1:  procedure lssRRts($\Theta_L^{ub}$, $t_{lmt}$)
2:    $pop_1 \leftarrow$ RandomBinarySequence($L$)
3:    Evaluate($pop_1$)
4:    $\Theta(\varsigma^*) \leftarrow$ ValueBest(pop)
5:    while $t < t_{lmt}$ and $\Theta(\varsigma^*) > \Theta_L^{ub}$ do
6:      $pop_1 \leftarrow$RandomBinarySequence($L$)
7:      $pop_1 \leftarrow$TabuSearch($pop_1$)
8:      Evaluate($pop_1$)
9:      $\Theta(\varsigma^*) \leftarrow$ ValueBest(pop)
10:   end while
11: end procedure
```

(b) lssRRts solver, based on reduction of lssMAts.

Figure 4: We illustrate two instrumented versions of the labs solver named as MA_{TS} in [30] under the caption "Pseudo code of the memetic algorithm", Figure 5. The instrumentation, highlighted with gray background, uses variable names defined in Table 1 and fits unobtrusively within the context of the original pseudo code: it is designed to control solver termination not only with a runtime limit but also by monitoring the solution quality in terms of a pre-specified upper bound. The procedure lssMAts on the left describes the actual solver in our experiments, adapted to solve instances of the labs problem only for odd values of L under skew-symmetry. A more general labs solver, for both even/odd values of L and also described by the same pseudo code, has been named lMAts. The procedure lssRRts on the right describes an alternative solver to lssMAts – it is also the name of the solver used in our experiments. While the solver on the left relies on an established evolutionary algorithm to initialize the tabu search, the modified solver uses randomly generated coordinates to initialize the tabu search. This set-up allows us to investigate the performance of the tabu search alone.

walk segments. The procedure `walk.saw` makes a contiguous self-avoiding walk segment as a sequence of best pivot coordinates, an arrangement formalized in Eq. 8. The procedure `newPivot.saw` searches the distance=1 neighborhood as defined in Eq. 7 for the best new pivot under the self-avoiding walk restrictions.

Since procedure `newPivot.saw` is the computationally most critical part of the solver, we provide additional details. The neighborhood search proceeds in randomized order (Step 3) to avoid inducing bias in the order of best pivot selection. The Step 5 eliminates all adjacent coordinates that may have been used as pivots already and returns a neighborhood subset $\mathcal{N}_{saw}(\varsigma_{\omega-1})$. To manage this search efficiently, we use a hash table to store pivot coordinates $Walk_\omega$. If the neighborhood subset is not empty, the procedure `bestNeighbor` in Step 7 probes all coordinates in the subset and returns the new pivot, updates the walk list to $Walk_\omega$ in Step 8, and exits on Step 16. An empty neighborhood implies that the self-avoiding walk is *trapped*, i.e. all adjacent coordinates are already pivots – an event not yet observed. We complete the procedure with Steps 11, 12, 13.

Solvers `lMAts`, `lssMAts` and `lssRRts`. Both solvers `lMAts` and `lssMAts` (Figure 4a) are instrumented versions of the `labs` solver named as MA_{TS} in [30]. These solvers, their pseudo code, and associated experiments and results, are described in [30]. Setting of control parameters in our experiments are identical to ones used in [30]; a consise reprise of these setting is shown in the top-right part of Figure 4. Our instrumentation is highlighted in gray. We also added the *cntProbe* variable which is not shown.

The solver `lssRRts` (Figure 4b) is a derivative of `lssMAts`; we devised it as a separate solver so we could investigate the performance of the tabu search, as implemented in `lssMAts`, without its evolutionary component.

Differences in `lssMAts` and `lssOrel`. A series of comprehensive experiments in the next section reveals significant differences between some of the solvers. Comparisons of most interest are between `lssMAts` and `lssOrel`. We

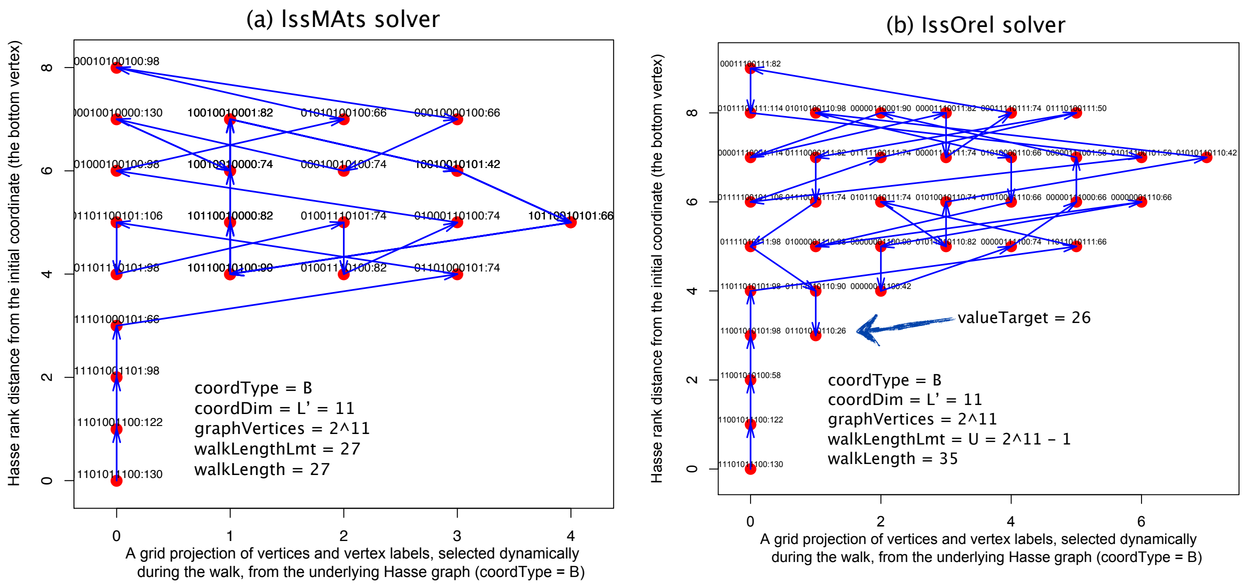

Figure 5: Two instances of walks created by two solvers, `lssMAts` and `lssOrel`.

conclude this section with an illustrative example which provides a modicum of explanation why such differences impact the asymptotic performance of both solvers.

Consider an instance of a `labs` problem for $L = 21$ where we take advantage of skew-symmetry to reduce the problem size to $L' = 0.5 * (L + 1) = 11$. The corresponding Hasse graph now has $2^{11} = 2048$ vertices and is too large to plot and trace edges from each vertex to 11 of its neighbor vertices and their labels directly. However, when walk lengths are on the order of 30–50 steps, we can project vertices and labels that have been visited in the underlying Hasse graph onto a uniform grid. In Figure 5 we display two instances of such projections, based on two different walks returned by two solvers, `lssMAts` and `lssOrel`: one walk terminates without finding the optimum solution, the other terminates upon finding the optimum solution, the pair 01101010110:26.

Both solvers start the respective walks from the same initial coordinate 11101011100, a substring of length $L' = 11$, which under rules of skew-symmetry expands into the full initial coordinate 111010111001101111101 of length $L = 21$ and `labs` energy value of 130. The labels associated with the initial vertex for each walk are given as the pair substring:value, starting with 11101011100:130. Both walks are shown in two grids: each grid represents a projection of vertices and vertex labels, selected dynamically during the walk, from the underlying Hasse graph. The length of the walk is prescribed by the solver.

Under Case (a), `lssMAts` selects the walk length *randomly* from the range $[L/2,\ 3L/2] = [\lfloor(L'-0.5)\rfloor,\ \lfloor(3L'-1.5)\rfloor] = [10,\ 31]$, and for the instance shown, the value of 27 has been selected. Under Case (b), `lssOrel` walk is limited only by the upper bound $2^{L'} - 1$. For this instance, `lssMAts` terminates the walk after step 27 without finding the solution target value and therefore needs to repeat the search from another coordinate. Moreover, the walk in `lssMAts` uses a tabu search strategy and is not self-avoiding in this instance: six vertices form a cycle 10010010000:74, 10010010001:82, 10010010101:42, 10110010101:66, 10110010100:90, 10110010000:82, and 10010010000:74. On the other hand, the self-avoiding walk in `lssOrel` continues for 35 steps and stops only upon finding the solution target value: 01101010110:26.

In each case, the walk length depends not only on the initial coordinate but also on the initial randomly selected seed. With `lssMAts` and the initial coordinate 11101011100, runs with 32 random seeds return walks of lengths in the range of [10, 31] where only 14 walks terminate at the target solution value of 26. With `lssOrel` and the initial coordinate 11101011100, runs with 32 random seeds return walks of lengths in the range of [4, 226] where *all* 32 walks terminate at the target solution value of 26.

Additional experiments can determine the more likely walk length means of each solver, with each reaching the same target value. Given one thousand randomly selected initial coordinates and random seeds for $L = 21$, the mean value of total walk length returned by `lssMAts` is 232.6 with the 95% confidence interval [214.1, 251.1]. This statistics has considerable bias since `lssMAts` has an advantage by relying on population of 100 randomly initialized solutions before proceeding with the search proper, thereby finding 167 solutions that reach the target value of 26 with walk length of 0 and 833 solutions that reach the target value with walk length > 0. Now, the mean value of total walk length returned by `lssMAts` based on 833 runs with walk length > 0 and under *multiple restarts*, is 279.2 with the 95% confidence interval [258.4, 300.1].

In comparison, when the same tests are applied to solver `lssOrel`, each of the one thousand walks terminate at the target value of 26 without a single restart: the mean value of walk length is 97.3 with the 95% confidence interval [93.6, 100.9]. This mean value is significantly better than

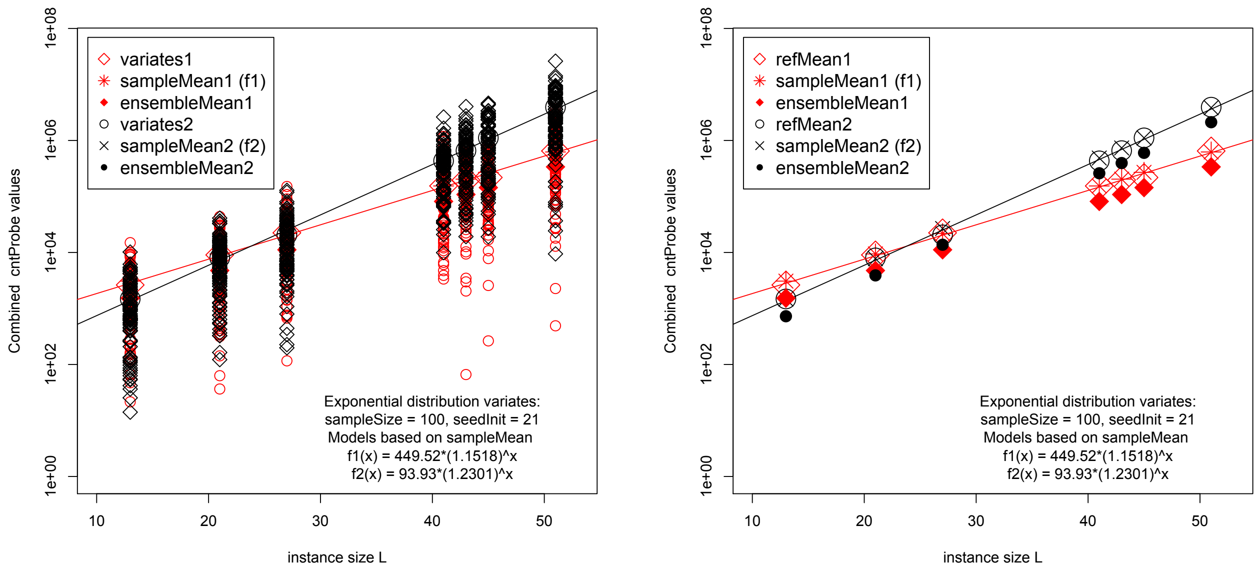

Figure 6: A simulated asymptotic performance evaluation of two `labs` solvers, given two reference models of *cntProbe* variable for the instance set $L = \{13, 21, 27, 41, 43, 45, 51\}$: $\text{ref1} = 500 * 1.150^L$ and $\text{ref2} = 100 * 1.230^L$. There are $N = 100$ variates generated by each model for each L, all variates have exponential distribution. Sample means are based on 100 variates for each L, values reported for ensemble means are based on the best-fit model with respect to all variates in the instance set. Due to exponential distribution of variates, sample means are not equivalent to ensemble means which we would expect under normal or uniform variate distribution. In all of our experiments that follow, we shall use sample means to model the asymptotic performance of various solvers. This experiment also demonstrates that with the sample size of 100, we can reliably model the asymptotic performance differences of two `labs` solvers.

the mean value of the Hamiltonian (self-avoiding) walk. Given that this instance has 4 minima, the mean value of the Hamiltonian walk is $(1/8)2^{11} = 256$. In conclusion, experiments with the instance shown in Figure 5 demonstrate that the solver which reduces the repetition of coordinates during the stochastic search more effectively also achieves a better average case performance. In comparison to `lssMAts`, `lssOrel` does requires more memory. In `lssMAts`, memory is required only to define the tabu data structure within the solution, the self-avoiding walk stores a path of already visited solutions. The experiments with `lssOrel` in the next section demonstrate a restart strategy with larger instances so that `lssOrel` memory remains fixed as well. However, as we show in our experiments, the self-avoiding walk outperforms the tabu search consistently and the gap widens as the instance size increases.

4. Summary of Experiments

We use the *asymptotic performance experiment* – as defined with a simulated experiment in Figure 6 – to reliably compare the performance of two `labs` solvers. By generating the asymptotic model for each solver, we not only readily compare the two solvers, we use the model also *to predict* computational requirements for maintaining *uncensored experiments* as the instances size increases – using also the metrics such as the *observed hit ratio* (Eq. 11). We follow this methodology consistently, under the given computational resources and time constraints [44].

We arrange our experiments into several groups. Given that the hardest-to-solve instances have only 4 minima – or equivalently a single canonic solution – when L is odd, we restrict the asymptotic performance experiments to this subset of L only. If during the experiment we find out that an instance has more than 4 minima, we exclude it from the test set. Similarly, when L is even, the hardest-to-solve instances have only two canonic solutions; we restrict the asymptotic performance experiments to this subset of L only. Given the available resources, including runtime, experiments that do not exploit the skew-symmetry of the labs function have been limited to $L \leq 87$. However, with solvers that do exploit the skew-symmetry, we could extend the experiments to $L \leq 401$.

When measuring *runtime* precisely is important, we perform experiments either on a PC or on a cluster of 22 processors [49], running under linux. In particular, we run the solver `lMAts` on the cluster where we control the processor load by running each solver instance serially – while also scheduling the runs on 22 processors in parallel. However, experiments with solvers `lssMAts`, `lssRRts`, and `lssOrel` on largest instances are scheduled in parallel and automatically on the grid with 100 processors, each solving an instance size of L under different random seeds and a *runtimeLmt* of 96 hours (4 days) for each instance. The PC has an Intel processor i7, clock speed of 2.93 GHz, cache of 8 MB, and main memory of 8 GB. The grid is a configuration of AMD Opteron processors 6272, clock speed of 2.1 GHz, cache of 2 MB, and main memory of 128 GB assigned to 64 cores [46]. When scheduled on the grid, processors run under variable load factors and direct comparisons of solver *runtime* are no longer possible. However, by instrumenting each solver with the counter such as *cnt-*

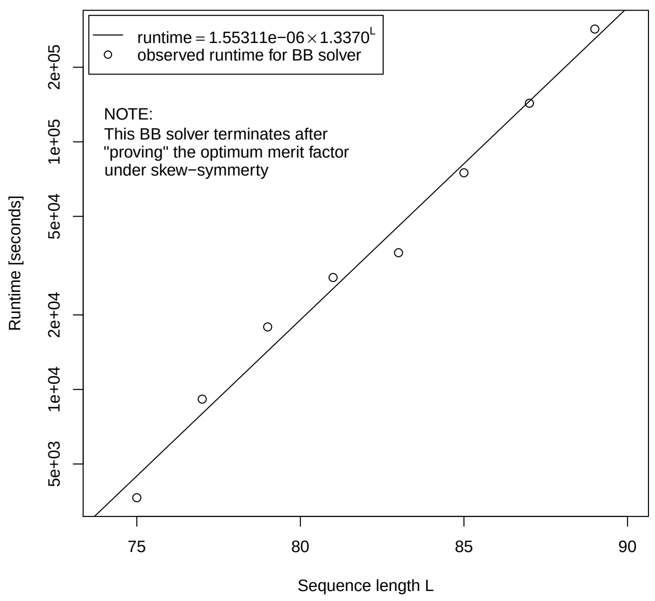

(a) branch-and-bound solver [20]

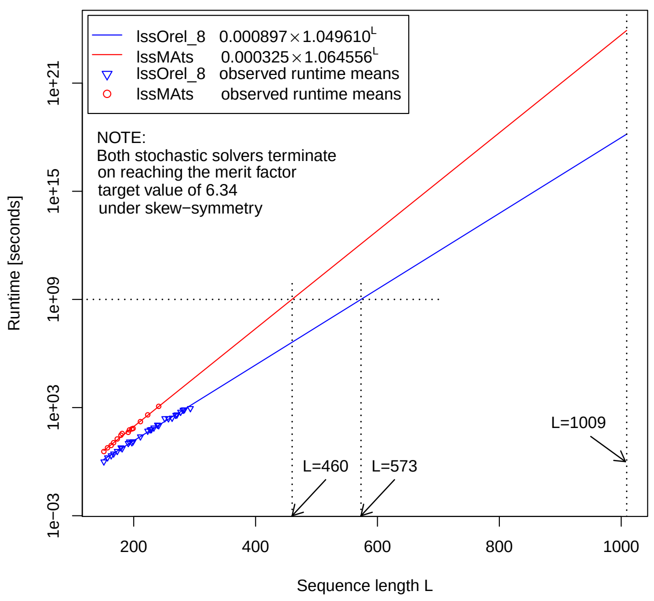

(b) `lssMAts` and `lssOrel_8` solvers

Figure 7: A runtime asymptotic comparison of the observed and projected performance of the state-of-the-art branch-and-bound `labs` solver under skew-symmetry [20] versus the observed and projected runtime of two stochastic solvers under skew-symmetry: `lssOrel_8` and `lssMAts`. In (a), the objective of the BB solver is to find (and prove) the optimal merit factor (under skew-symmetry) for increasing values of L; the solution for $L = 89$ reports a runtime of 285326 CPU seconds whereas solvers `lssOrel_8` and `lssMAts` reach the same merit factor in 1.6869 and 3.2774 seconds on the average, with each average based on 100 *uncensored* trials. The primary objective in (b) is to determine the asymptotic runtime performance of the two stochastic solvers while searching for sequences with the merit factor of 6.34: such sequences can be readily found experimentally with constructive methods [33, 34]. Experimental results in Figure 15a demonstrate that for $L = 1009$, the merit factor of approximately 6.34 can be reached in less than 1 CPU second while for $L = 4021$, a solution with comparable merit factor takes about 72 CPU seconds. With stochastic solvers, computational bottlenecks are observed already for $L > 400$: the *observed average runtimes* (based on 100 uncensored trials) with `lssOrel_8` rise from 103 CPU seconds at $L = 241$ to 910 CPU seconds for $L = 293$ while `lssMAts` requires 1142 CPU seconds on the average to reach 6.34 at $L = 241$. By extrapolation, finding solutions with merit factor 6.34 for $L = 573$ requires $O(10^9)$ seconds or around 32 years with `lssOrel_8`, whereas with `lssMAts` solutions of comparable quality are expected for $L = 460$ in the same time frame. For the large value of $L = 1009$, the average runtime prediction to reach the merit factor of 6.34 with for `lssOrel_8` is 46774481153 years – which exceeds the current estimate about the age of the universe by a factor of 3.4. This explains why the best reported merit factor with solver `lssOrel_8`, valued at 8.0668 for $L = 241$ in Figure 13, is almost surely not optimal.

Probe, solver performance comparisons remain platform-independent. Note that this is only the case when the cost of the evaluation function is the same for all solvers and the evaluation function is the most compute-intensive method. Both of these criteria are satisfied in our experiments.

Before proceeding to details of experiments about individual solvers, we pause to make a realistic assessment about the runtime complexity of the `labs` problem in terms of observed and extrapolated experimental results in Figure 7. In contrast to the branch-and-bound solver searching for an optimal merit factor, the stochastic solvers `lssOrel_8` (number 8 determines the maximum length of the self-avoiding walk segment $\omega_{lmt} = \omega_c * \frac{L+1}{2}$, where $\omega_c = 8$) and `lssMAts` search for sequences with the merit factor of 6.34: such sequences can be produced in polynomial time with constructive methods [33, 34]. The most important observations to infer from Figure 7 are: (1) runtime performance of branch-and-bound solver is inadequate to solve instances that are of current interest; (2) both stochastic solvers start exhibiting computational bottlenecks for $L > 400$ even when the merit factor target values are relaxed and far from the best values. Neither `lssOrel_8` nor `lssMAts` and least of all, the branch-and-bound solver, can be expected to find the conjectured optimal merit factors without faster computers and massive parallelism.

The best course of action at this time is to systematically learn about limitations of current solvers and to continue with summaries of the following experiments: (1) solver `lMAts` for L_{odd} and L_{even}, (2) best upper bounds of L_{odd} without skew-symmetry, (3) solver `lssOrel_U` (each solution is based on a single segment contiguous walk), (4) solver `lssOrel` with limited walk length, (5) solver `lssOrel_U` versus `lssOrel_8`, (6) solver `lssMAts` versus `lssRRts`, (7) solver `lssOrel_8` versus `lssMAts`, including asymptotic predictions and hit ratios, and (8) solver `lssOrel_8` versus best known merit factors in the literature and *new best-value solutions* of the `labs` problem, (9) challenges for the next generation of labs solvers, the asymptotic view.

(1) Experiments with `lMAts`. Experiments with solver `lMAts` have been designed to illustrate its asymptotic performance; we summarize it in Figure 8 and in Table 3. We consider two specific subsets of sequence lengths L:

$$L_{odd} = \{13, 21, 27, 41, 43, 45, 51, 57, 71, 77, 83, 87\} \quad (22)$$

$$L_{even} = \{20, 24, 28, 32, 34, 36, 38, 40, 42, 44, 48, 52, \quad (23)$$
$$54, 58, 60, 62, 64, 66, 68, 74, 76, 78, 80, 82, 84, 86\}$$

For values of L in the subset L_{odd} there are only four optimal solutions, which reduce to a *single canonic solution* – making these instances hardest-to-solve. For values of L in the subset L_{even} there are only eight optimal solutions, which reduce to a *canonic solution pair* – making these instances hardest-to-solve for even values of L. There are four plots in Figure 8:

(a) Predictor models for observed sample mean of *cntProbe*

$$\begin{aligned} cntProbe(\texttt{lMAts})_{odd} &= 320.360 * 1.3421^L \quad (24)\\ cntProbe(\texttt{lMAts})_{even} &= 114.515 * 1.3464^L \end{aligned}$$

(b) Predictor models for observed sample mean of *runtime* (converted from seconds in the figure to hours here)

$$\begin{aligned} runtime(\texttt{lMAts})_{odd} &= 1.832 * 10^{-8} * 1.3421^L \quad (25)\\ runtime(\texttt{lMAts})_{even} &= 6.671 * 10^{-9} * 1.3464^L \end{aligned}$$

(c) Observed *hit ratio* as defined in Eq. 11. For *runtimeLmt* = 10 hours, we can observe the *hit ratio* of 100% up to $L = 57$ for odd values of L and up to $L = 64$ for even values of L. This implies that under current *runtimeLmt* we can not reliably measure average-case performance of solver `lMAts` for larger values of L.

(d) The solver `lMAts` significantly outperforms the two earlier stochastic solvers, `ES` and `KL` [25, 26]. Note that the observed values of *cntProbe*, which are platform-independent, are still relevant 11 years after the initial experiments: $cntProbe(\texttt{ES})_{odd} = 5.76855 * 1.5097^L$ and $cntProbe(\texttt{KL})_{odd} = 50.9714 * 1.4072^L$. Our current estimates of asymptotic performance are more accurate, since we process observations not as single ensemble but as two ensembles, one for odd and the other for even values of L.

More about Figure 8. Predictor models for *cntProbe* and *runtime* are based on a sample size of 516. The model mean is only an approximate predictor of the observed sample mean – it can underestimate as well as overestimate. For $L = 57$, the observed runtimes range from 2 seconds to slightly more than 2 hours, with the sample mean of 1340.4 seconds. However, when we report on sample means over five consecutive intervals, with 100 samples in each interval, sample means range from 1155.3 seconds to 1624.9 seconds – as anticipated in Eq. 15.

For this series of experiments we had access to a cluster of 22 *unloaded processors* and could schedule executions in parallel while still measuring runtimes that would be consistent with runtimes we would observe serially on a single unloaded processor. Since runtime measurements under 1 seconds are not precise even for an unloaded processor, we rely on near 100% correlation with *cntProbe* and compute *runtime* indirectly for all values of L.

Predictions and observations in Table 3. We relate observations from experiments with `lMAts` to *observed hit ratio*, *predicted hit ratio*, and runtime models as defined by Eqs. 10, 16, and 26. The rapid decline in observed *hit ratio*, under the constraint of *runtimeLmt* of 10 hours can also be observed/predicted in this table and in Figure 8c. The experiments with solver `lMAts` define the methodology when focusing on the performance of solvers `lssOrel` and `lssMAts` under skew-symmetry. Again, we define groups for L_{odd} to arrange the sequence of our experiments.

(2) Best upper bounds pairs for L_{odd}. The experiments with `lMAts` show the importance of (a) separating instances for L_{odd} from instances for L_{even}, and (b), separating instances in both L_{odd} and L_{even} into additional groups: a group with single canonic solution for L_{odd}, a group with a single pair canonic solutions for L_{even}, and groups with more canonic solutions. For experiments that follow for L_{odd}, we again define the hardest-to-solve instances as having a single canonic solution, and divide them into two groups, primary and secondary:

$$L_{prim} = \{5, 7, 11, 13, 21, 27, 41, 43, 45, 51, 57,$$
$$71, 77, 83, 91, 95, 97, 99, 101, 103, 105\} \quad (26)$$

$$L_{secd} = \{71, 77, 83, 91, 95, 97, 99, 101, 103, 105,$$
$$107, 109, 111, 115, 117, 119, 121, 123, 125, 127\} \quad (27)$$

The instance $L_{prim} = 105$ is the largest instance where the solver `lssOrel` does not exceed the maximum memory limit of 8 GB on our PC and completes as *uncensored* a self-avoiding walk without a single restart from each randomly assigned initial coordinate. We observe a single canonic solution for each value of L in this group, so we can formulate an asymptotic predictor model based on sample means, similarly to Eqs. 25 and 26. The instance $L_{secd} = 127$ is the largest instance where the solver `lssOrel` completes 100 *uncensored* performance evaluations (initialized with 100 random seeds) within 2 days ($\sum_{i=1}^{100} runtime_i < 2\ days$) on our PC; i.e. observing a *hit ratio of 100%* and returning a mean value for the sample size of 100. Again, we observe a single canonic solution for each value of L in this group, so again we can formulate an asymptotic predictor model based on sample means.

For the remainder, we consider the tertiary group, with all experiments performed on the grid [46].

$$L_{tert} = \{141, 151, 161, 181, 201, 215, 221, 241, 249,$$
$$259, 261, 271, 281, 283, 301, 303, 341, 381, 401\} \quad (28)$$

We place $L_{tert} = 141$ into the tertiary group since the number of observered canonical solutions is greater than 1. The instance $L_{tert} = 151$ is the smallest instance where

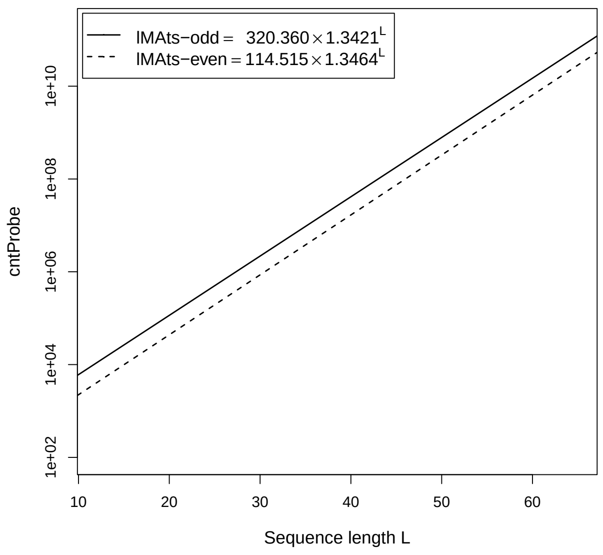

(a) The sample mean asymptotic model for *cntProbe*.

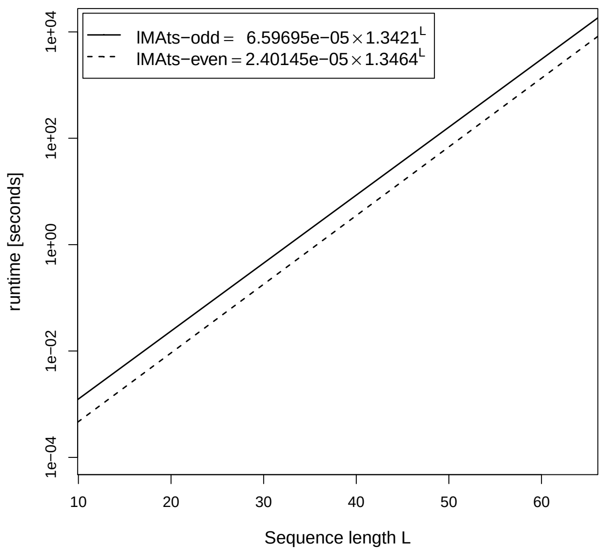

(b) The sample mean asymptotic model for *runtime*.

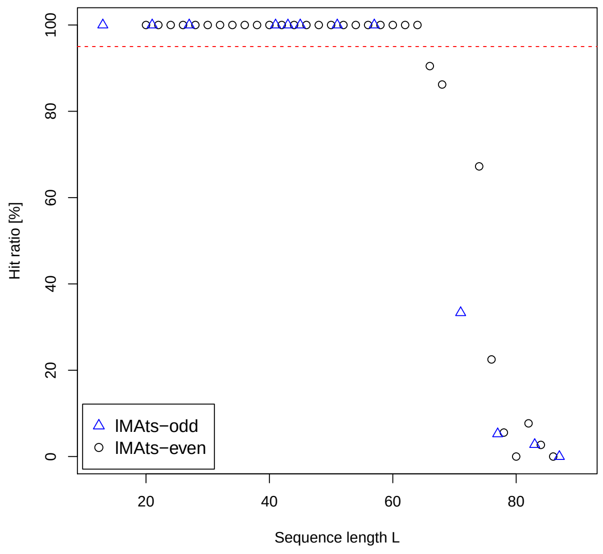

(c) For runtimLmt=10 hours and $L \leq 64$, hitRatio=100%.

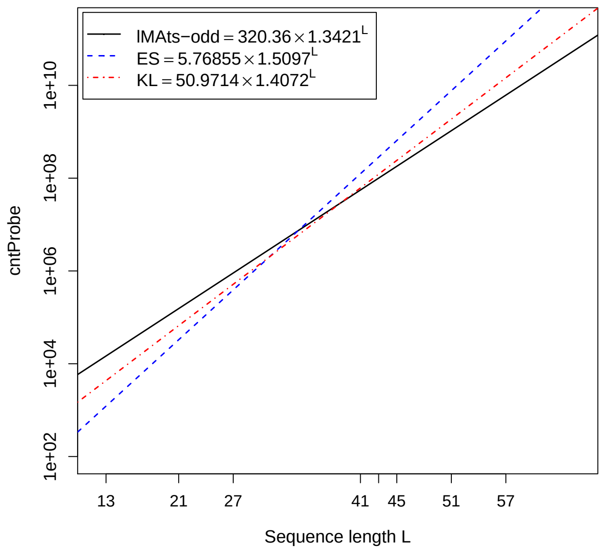

(d) Asymptotic comparisons to earlier solvers [25, 26].

Figure 8: The asymptotic performance of solver `lMAts` for sequence lengths L from the subsets L_{odd} and L_{even}. As expected, instances from L_{odd} take significantly more time to solve than instances from L_{even}. The sample mean asymptotic models are based on sample size $N = 516$ and rely only on runtime samples of L where runtime is not censored, i.e. for hitRatio = 100%. For consistency with observed hitRatio in Table 3, the plot of hitRatio in this Figure also relies on the sample size of 100. Finally, the solver `lMAts` significantly outperforms the two earlier stochastic solvers, `ES` and `KL` from [25, 26]. Here, the performance is measured not in *runtime* but the observed values of *cntProbe* which are platform-independent and as such, still relevant 11 years after the initial experiments.

we no longer observe a hit ratio of 100% with the solver `lssOrel` within *runtimeLmt* = *4 days*. With exception of $L_{tert} = 141$, solutions in this group associate with *a distribution of merit factors* rather than a single best value; see Table 5 and Figure 14 later in this section. For these instances, we can only report the best figure of merit; the probability that the associated sequence is either optimal or near-optimal is almost 0 as the instance size increases.

See Table 4 for a summary of best known upper bound values on `labs` energies for given subsets of L_{odd}. Up to $L = 99$, these energies are listed as pairs: the first number represents the best value achieved under coordinates with skew-symmetry, the adjacent number in brackets gives the number of canonic solutions under skew-symmetry. The second number represents the best value achieved with coordinates that are not skew-symmetric; the adjacent number in brackets gives the number of canonic solutions that are not skew-symmetric. In 2002, Knauer posted the ‘best-value solutions’ for $L > 101$ without the restriction of skew-symmetry [19]; results in Table 4 show that our

Table 3: Predictions versus observations from experiments with `lMAts`, under the constraint of *runtimeLmt* of 10 hours for the listed values of L, each with the sample size of 100. For L odd, we only consider hardest-to-solve instances, each having a single canonic solution. For L even, we also consider the hardest-to-solve instances, each having two canonic solutions. The observed mean represents the sample mean based on the value of observed solvability, i.e. the sum total of runtimes of each instance. The *observed number of hits*, $hitO = 100$, signifies that none of the solutions have been censored. The model mean values are computed from the two predictors based on empirical data described in Figure 8. The values of predicted solvability, computed from Eq. 20, are waiting times to reach *hitRatio* of 100% with probability of 0.99 – provided (1) the solver has been scheduled on a single processor to invoke on each instance serially, and (2) the solution produced by the solver has not been censored.

(a) L is odd

L	model mean*	observed mean	predicted solvability†	observed solvability	*hitO*‡
57	0.3521	0.3734	43.92	37.34	100
71	21.66	8.345	2702	834.5	33
77	126.6	9.686	15791	968.6	5
83	739.9	9.887	92284	988.7	3
87	2400	10.0	299412	1000	0

* runtime(`lMAts`)$_{odd} = 1.832 * 10^{-8} * 1.3421^L$
† in hours, using Eq. 20; $N = 100, p = 0.99$
‡ using Eq. 10

(b) L is even

L	model mean*	observed mean	predicted solvability†	observed solvability	*hitO*‡
58	0.2071	0.2993	25.83	29.93	100
60	0.3755	0.2656	46.83	26.56	100
62	0.6807	0.4877	84.90	48.77	100
64	1.233	1.167	153.9	116.7	100
66	2.236	3.502	279.0	350.2	90
68	4.055	4.264	505.7	426.4	86
74	24.15	6.355	3013	635.5	67
76	43.79	9.242	5461	924.2	23
78	79.38	9.829	9901	982.9	5
80	143.9	10.0	17949	1000	0
82	260.8	9.475	32538	947.5	7
84	472.9	9.817	58984	981.7	3
86	857.3	10.0	106927	1000	0

* runtime(`lMAts`)$_{even} = 6.671 * 10^{-9} * 1.3464^L$

skew-symmetry solver `lssOrel` consistently returns improved skew-symmetric solutions vis-à-vis Knauer's solutions without skew-symmetry, and then a few more.

(3) Experiments with `lssOrel_U`. The experiments with `lssOrel_U` for 14 hardest-to-solve instances are summarized in subfigures 9a-9-d; they range from $L = 41$ to $L = 105$. Note the high correlation of *cntProbe* versus *runtime* and *walkLength* versus *cntProbe*: for all values of L, this correlation remains at about 99%.

The letter `U` in the solver name is a parameter that stands for *unlimited length of the self-avoiding walk segment* in contrast to `lssOrel_8` where `8` stands for the value of walk segment coefficient ω_c that determines the maximum length of the self-avoiding walk segment $\omega_{lmt} = \omega_c * \frac{L+1}{2}$, already defined in Table 1; `lssOrel_8` is discussed in more details later.

Under the walk segment coefficient value of `U`, solver `lssOrel` invokes the procedure WALK.SAW in Figure 3 only once; the walk is contiguous and terminates as a single segment only upon reaching the upper bound Θ_L^{ub}. For $L = 105$, the largest instance reported in this group of experiments, we have $\Theta_{105}^{ub} = 620$. In our experiments with $L = 105$ we record instances of 100 distinct single-segment contiguous walks, each starting at a different randomly selected coordinate and random seed, with each walk terminating at one of the four solution coordinates with the best-known value of 620. We have not observered a single instance of a trapped pivot that would induce a restart of another walk segment. The *runtime*, *cntProbe* and and *memory footprint* range from 0.04 to 278.87 seconds, $2^{18.66}$ to $2^{31.21}$ probes and 2.2 MB to 1.97 GB, respectively. The averages for *runtime*, *cntProbe*, *walkLength*, and *memory footprint* are 72.48 seconds, $2^{29.28}$ probes, $2^{23.59}$ steps, and 0.516 GB, respectively. We could not run instances of size $L = 107$ without a single restart due the 8 GB memory limit of our PC.

In lattices, with grid structures that are simpler when compared to our Hasse graphs, physicists continue to push the envelope on the maximum length of self-avoiding walks: experiments with *longest walks under 64 GB of memory* are reported as having maximum lengths of $2^{28}-1$ in a 3D lattice and $2^{25}-1$ in a 4D lattice [43].

The predictor models for observed sample means of *cntProbe* and *runtime* (in seconds) are

$$\begin{aligned} cntProbe(\texttt{lssOrel\_U}) &= 73.05 * 1.1668^L & (29)\\ runtime(\texttt{lssOrel\_U}) &= 1.8 * 10^{-6} * 1.1846^L & (30)\end{aligned}$$

Of these two models, only the predictor for *cntProbe* is platform independent, the predictor for *runtime* (in seconds) is valid for the specified PC only. Similarly to Eq. 26, we compute coefficients in *runtime*(`lssOrel_U`) indirectly by taking advantage of the high correlation between *cntProbe* versus *runtime*.

Results obtained with `lssOrel_U` provide the baseline for all experiments that follow.

(4) Solver `lssOrel` under limited walk length. The length of the self-avoiding walk segment is controlled by the walk segment coefficient ω_c: $\omega_{lmt} = \omega_c * \frac{L+1}{2}$, see Table 1. The value of ω_c extends the name of the solver `lssOrel`, for example `lssOrel_8` can be interpreted, in the case of $L = 105$, as limiting the contiguous walk length to a maximum of $\omega_{lmt} = 8 * 53 = 424$ steps.

Under the limited walk length, solver `lssOrel` invokes the procedure WALK.SAW in Figure 3 with a randomly selected initial coordinate a number of times, creating the

Table 4: Pairs of best upper bound values on `labs` energies for a subset of odd values of L. The first number is the best value achieved under coordinates with skew-symmetry; the adjacent number in brackets gives the number of canonic solutions under skew-symmetry. The second number is the best value achieved with coordinates that are not skew-symmetric; the adjacent number in brackets gives the number of canonic solutions that are not skew-symmetric. The significance is this: solutions under skew-symmetry can be equivalent to solutions without skew-symmetry. Entries such as **15**(2)/–, **26**(1)/–, etc. imply that for $L = 15$, $L = 21$, etc. *all* solutions are skew-symmetric; the ones of most interest in this group are solutions where the number of canonic solutions is 1, forming *a primary group*: $L = 5, 7, 11, 13, 21, 27, \ldots$. For $L \geq 101$, all solution values represent the 'best-known values under skew-symmetry'. Values marked with * are an improvement on values posted by Knauer in 2002, now accessible under [50]. We make no attempt to find new and improved solutions for all values of L in [19], except to show that solver `lssOrel` consistently returns improved skew-symmetric solutions vis-à-vis Knauer's solutions without skew-symmetry. For details, see Table 6 in Section 4. Entries shown as '?' imply that no 'best solutions' have been reported at this time.

L	**1**	**3**	**5**	**7**	**9**
0	–	–	**2**(1)/–	**3**(1)/–	**12**(2)/12(4)
10	**5**(1)–	**6**(1)/–	**15**(2)/–	**32**(1)/32(10)	33(2)/29(2)
20	**26**(1)/–	51(4)/47(6)	52(1)/36(2)	**37**(1)/–	**62**(2)/–
30	79(1)/67(2)	88(2)/64(2)	89(2)/73(2)	106(1)/86(2)	**99**(2)/–
40	**108**(1)/–	**109**(1)/–	**118**(1)/–	**135**(5)/135(2)	**136**(1)/136(2)
50	**153**(1)/–	**170**(1)/170(1)	**171**(2)/–	**188**(1)/–	**205**(1)/205(2)
60	230(1)/226(2)	271(3)/207(2)	272(4)/240(2)	**241**(3)/241(2)	282(1)/274(1)
70	**275**(1)/-	348(2)/308(2)	341(1)/329(2)	**358**(1)/–	407(5)/339(1)
80	400(1)/372(1)	**377**(1)/–	442(1)/414(1)	451(1)/431(1)	484(2)/432(1)
90	**477**(1)/–	502(3)/486(1)	**479**(1)/–	**536**(1)/536(1)	**577**(1)/–
100	578(1)	555(1)	620(1)	677(1)	662(1)
110	687(1)	752(2)	745(1)	786(1)	835(1)
120	844(1)	893(1)	846(1)	887(1)	920(1)
130	913(1)	1010(1)	1027(1)	1052(1)	1133(1)
140	1126(2)	1191(1)	1208(1)	1265(2)	1218(1)
150	1275(4)	1340(1)	1437(1)	1366(1)	1439(1)
160	1512(2)*	1529(1)	1474(1)	1563(1)	1532(1)
170	1677(1)	1598(1)*	1687(1)*	1648(1)*	1761(1)*
180	1834(1)*	1859(2)*	2028(1)	1973(1)	1966(1)
190	2191(1)	2272(1)	2281(1)	2218(1)	2275(1)
200	2380(1)*	2421(1)	2662(1)	2695(1)	2664(1)
210	2801(1)	2698(1)	2691(1)*	3036(1)	3189(1)
220	2758(1)*	3215(1)	3416(1)	3409(1)	3474(1)
230	3587(1)	3692(1)	3757(1)	3590(1)	3711(1)
240	3600(1)*	4073(1)	4098(1)	4291(1)	3812(1)*
250	4165(1)	4382(1)	4463(1)	4472(1)	4145(1)*
260	4338(1)*	4803(1)	4948(1)	5037(1)	4950(1)
270	4871(1)*	?	?	?	?
280	5260(1)*	5333(1)*	5790(1)	?	?
300	6054(1)	6335(1)*	?	?	?
340	8378(1)	?	?	?	?
380	10238(1)	?	?	?	?
400	11888(1)	?	?	?	?

The *primary group* of the hardest-to-solve instances includes the following values of L: $\{5^\dagger, 7^\dagger, 11^\dagger, 13^\dagger$, 21, 27, $41^\dagger$, $43^\dagger$, 45, 51, 57, $71^\dagger$, 77, $83^\dagger$, 91, 95, $97^\dagger$, 99, $101^\dagger$, $103^\dagger$, $105\}$. The instance $L = 105$ is the largest instance where the solver `lssOrel` does not exceed the maximum memory limit of 8 GB and completes as *uncensored* a self-avoiding walk without a single restart from each randomly assigned initial coordinate.

The *secondary group* of the hardest-to-solve instances includes the following values of L: $\{71^\dagger$, 77, $83^\dagger$, 91, 95, $97^\dagger$, 99, $101^\dagger$, $103^\dagger$, 105, $107^\dagger$, $109^\dagger$, 111, 115, 117, 119, 121, 123, 125, $127^\dagger\}$. The instance $L = 127$ is the largest instance where the solver `lssOrel` completes 100 *uncensored* performance evaluations (initialized with 100 random seeds) within 2 days on our PC.

The *tertiary group* in our testing includes instances with the following values of L: $\{141$, $151^\dagger$, 161, $181^\dagger$, 201, 215, 221, $241^\dagger$, 249, 259, 261, $271^\dagger$, $281^\dagger$, $283^\dagger$, 301, 303, 341, 381, $401^\dagger\}$. Here, the solver `lssOrel` reports on the best bound returned in 4 days of computing under random initial seeds on 100 CPU units.

Values marked with † are prime numbers.

Finally, not all solutions with coordinates that are skew-symmetric are also optimal: such solutions have been observed for L = 19, 23, 25, 31, 33, 35, 37, 61, 63, 65, 69, 73, 75, 79, 81, 85, 87, 89 and 93.

walk as a sequence of contiguous self-avoiding walk segments. However, since each walk segment is independent, there is no need to store the previous walk segments. Thus, the walk segment coefficient determines not only the maximum walk length of the contiguous self-avoiding walk segment but also the amount of memory needed to store the current segment.

To find out the effect of the limited walk length on solver, we ran experiments with the secondary group of the hardest-to-solve instances (Eq. 27, see also Table 4) with walk segment coefficient values set to $\omega_c = 1$, 2, 4, 8, and 16 – see subfigures 9e-9-f. These results demonstrate that solver `lssOrel_8` exhibits the best asymptotic average-case performance with *cntProbe* of $650.07 * 1.1435^L$. The second and third best results are achieved with $\omega_c = 16$ and 4 while the worst results are achieved with $\omega_c = 1$. For example, consider the case of $L = 127$: by changing $\omega_c = 1$ to $\omega_c = 8$, the mean value of *cntProbe* decreases from $2^{34.64}$ to $2^{33.83}$, a decrease by a factor of 1.76.

Since experiments show that the effectiveness of `lssOrel` is best for the walk segment coefficient value of $\omega_c = 8$, we shall use `lssOrel_8` as the reference solver for comparisons with all other solver configurations in the remainder of this paper.

(5) Comparisons of `lssOrel_U` and `lssOrel_8`. The main difference between `lssOrel_U` and `lssOrel_8` is the walk segment length and consequently, the memory usage. See Figure 10 for experiments with 14 hardest-to-solve instances, ranging from $L = 41$ to $L = 105$. Results show (a) *cntProbe*, (b) *runtime*, (c) *speed*, and (d) memory usage. The solver speed is defined as the number of function evaluations (probes) per second. For $L < 71$ *runtime* is close to 0 and the speed cannot estimated accurately, hence results are shown for $L \geq 71$ only. The memory usage in Figure 10d is not an average value, it is the maximum memory usage observed for one of the 100 samples.

When observing *cntProbe* alone, the solver `lssOrel_U` has a slight advantage over `lssOrel_8` – which we would expect. However, as L increases, this advantage decreases for *runtime* – due to the increased reduction in speed observed for `lssOrel_U`. A significant factor in this speed reduction for `lssOrel_U` is the increasing memory require-

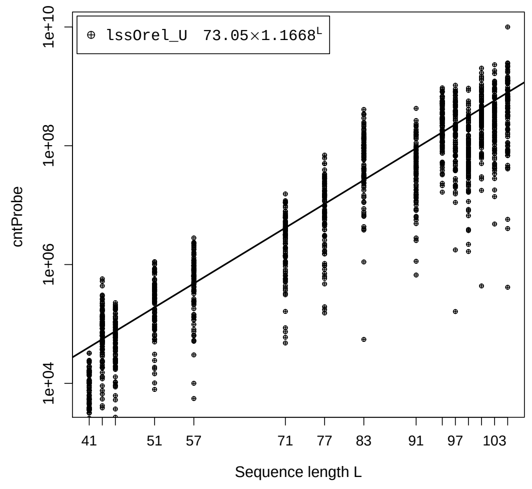

(a) L versus *cntProbe*

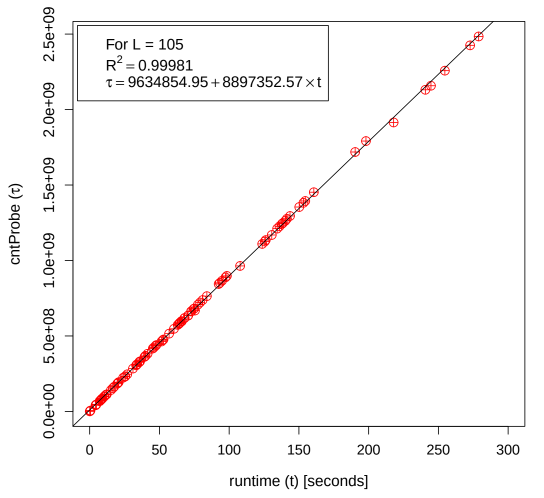

(b) Correlating *runtime* to cntProbe

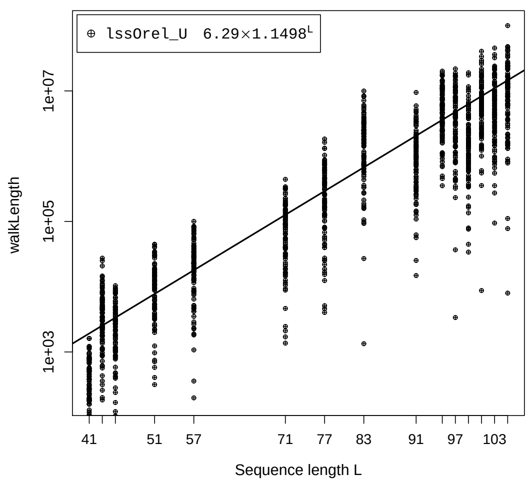

(c) L versus *walkLength*

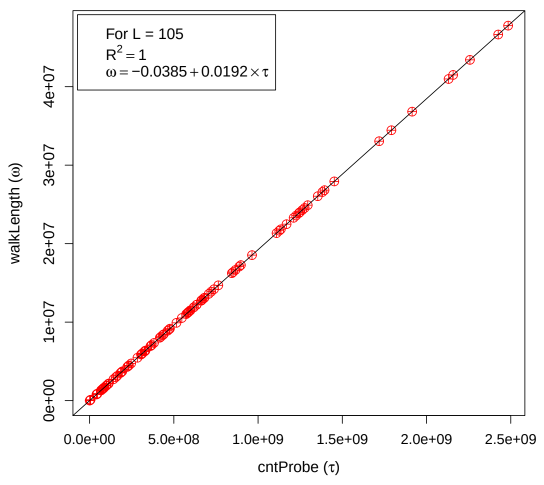

(d) Correlating *cntProbe* to walkLength

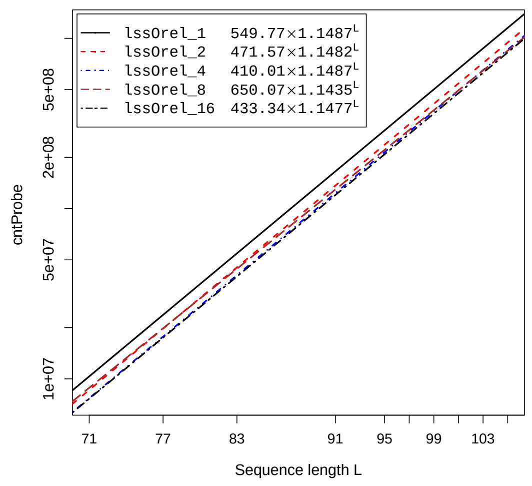

(e) Results for $L = 41$ to $L = 105$

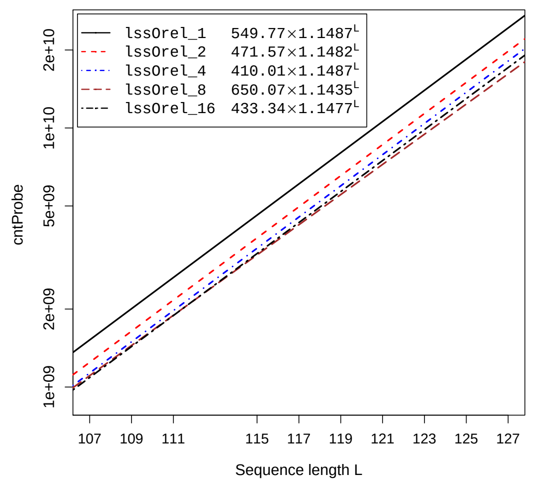

(f) Results for $L = 107$ to $L = 127$

Figure 9: Asymptotic performance of solvers `lssOrel_U` (a-d) and `lssOrel_`ω_c for walk length coefficients $\omega_c \in \{1, 2, 4, 8, 16\}$ (e-f). The best solver performance is achieved for $\omega_c = 8$. The values of $L = \{41, 43, 45, 51, 57, 71, 77, 83, 91, 95, 97, 99, 101, 103, 105, 107, 109, 111, 115, 117, 119, 121, 123, 125, 127\}$ represent the subset of hardest-to-solve instances of the `labs` problem; see Eq. 26 and Table 4. All predictor models in the form of $(a * b^L)$ are based on a sample size of $N = 100$.

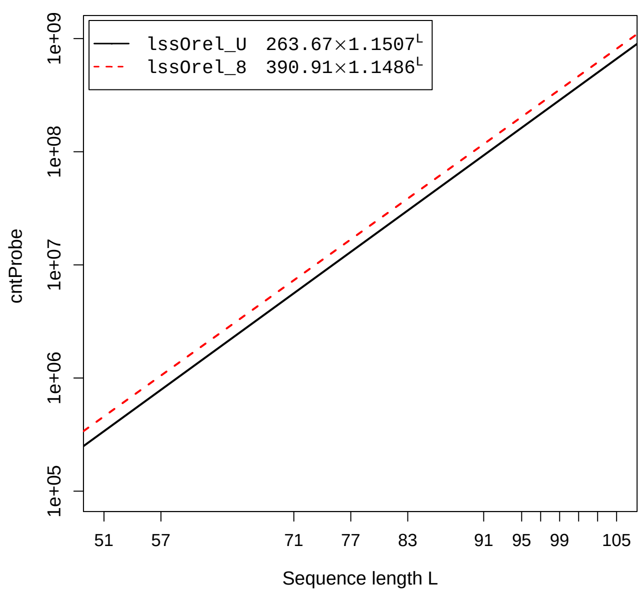

(a) *cntProbe* for $L = 51$ up to $L = 105$.

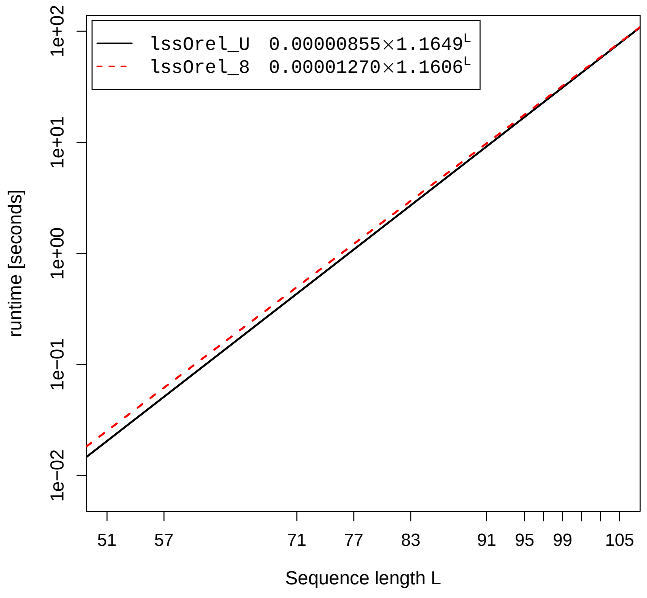

(b) *runtime* in seconds for $L = 51$ up to $L = 105$.

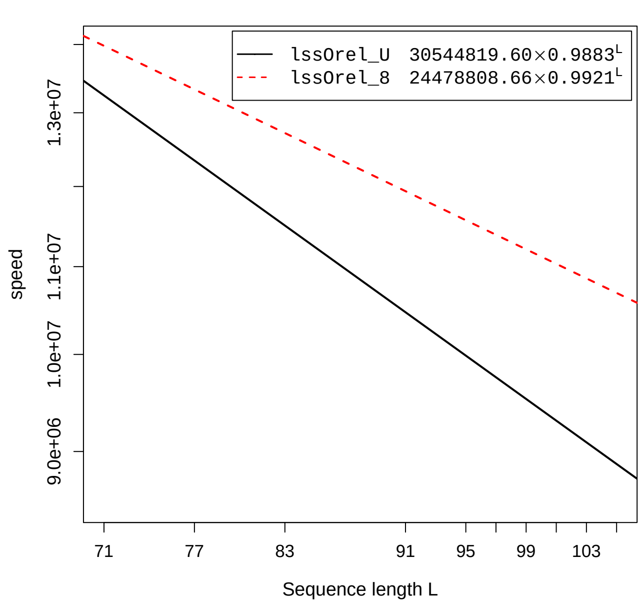

(c) *speed* for $L = 71$ up to $L = 105$.

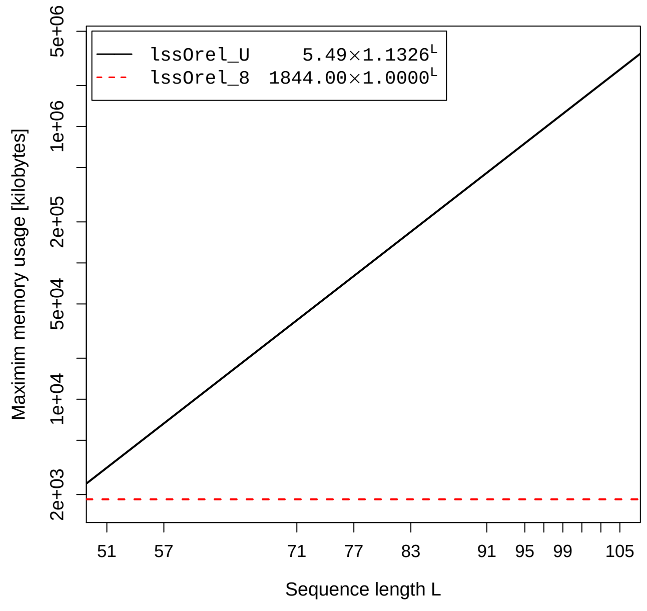

(d) Maximum memory usage for $L = 51$ up to $L = 105$.

Figure 10: Asymptotic comparison between two solvers: `lssOrel_U`, based on a single segment self-avoiding walk and `lssOrel_8` with walk composed of several self-avoiding segments, each of length fixed at $\omega_{lmt} = 8 * \frac{L+1}{2}$. As expected, the solver `lssOrel_U` has a slight advantage over `lssOrel_8` when we observe *cntProbe* only. However, the probability of a hash collision to maintain a self-avoiding walk under a fixed memory limit also increases with increasing L – which accounts for the observed reduction in speed of the solver `lssOrel_U`, and the approaching crossover in *runtime* when compared to `lssOrel_8`. A compromise solver, with only a modest memory requirement, such as `lssOrel_8` is needed for solving larger instance sizes.

ment for `lssOrel_U`, inducing an increased probability of a hash collision to maintain a self-avoiding walk under a fixed memory limit. As shown in the graph, the memory required by `lssOrel_U` increases with the instance size L while `lssOrel_8` requires a constant amount of memory, about 1.8 MB in our case.

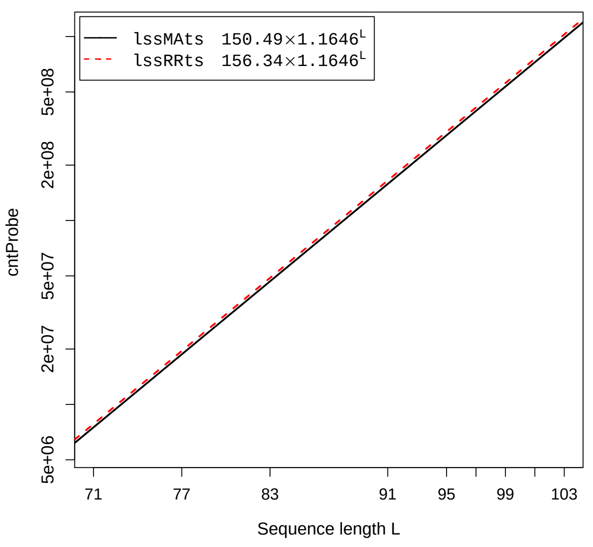

(a) Results for $L = 71$ up to $L = 105$.

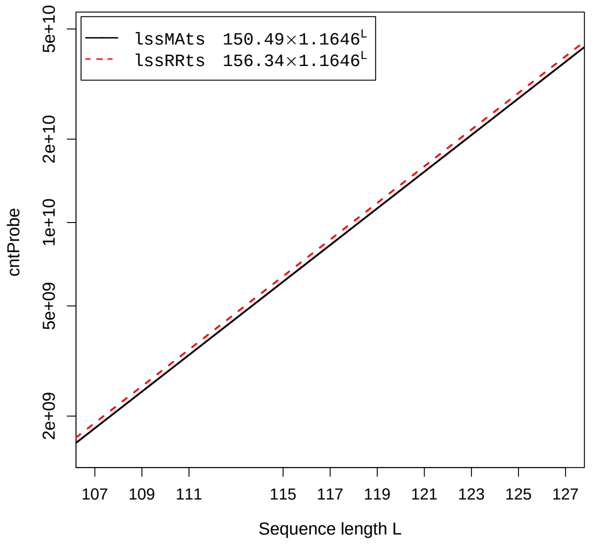

(b) Results for $L = 107$ up to $L = 127$.

Figure 11: Comparison between solvers `lssMAts` and `lssRRts`. We observe that the asymptotic average-case performance of these two solvers are statistically equivalent. Thus, for the labs problem, the evolutionary component within `lssMAts` is not effective.

What we learned from these experiments is that the solver such as `lssOrel_U` cannot deliver solutions under a single self-avoiding walk segment when the required walk length exceeds the available memory constraints of the solver – a compromise solver such as `lssOrel_8` is needed for solving larger instance sizes.

(6) Comparisons of `lssMAts` and `lssRRts`. The solver `lssRRts` is a derivative of `lssMAts`; asymptotic comparison of the two solvers is expected to reveal whether or not the initialization of tabu search by the evolutionary component within `lssMAts` significantly improves the solver performance in comparison with `lssRRts` where tabu search is initialized with a random binary sequence.

We ran experiments with the secondary group of the hardest-to-solve instances (Eq. 27, see also Table 4). The settings of `lssMAts` are the same as described in [30] and also shown in Figure 4. The solver `lssRRts` has only one control parameter: the tabu search walk length, set in the same way as `lssMAts`. Results are shown in Figure 11. We conclude that the asymptotic average-case performance of these two solvers are statistically equivalent. For the range $71 \le L \le 127$ we find *cntProbe* as $150.49 * 1.1646^L$ for `lssMAts` and $156.34 * 1.1646^L$ for `lssRRts`. Thus, for the `labs` problem, the evolutionary component within `lssMAts` is not effective.

(7) Comparisons of `lssOrel_8` and `lssMAts`. We ran two sets of experiments to compare the two solvers. With the first set, we measure the asymptotic average-case performance, with hardest-to-solve instances from the secondary group in Eq. 27. For the second set, we select 7 instances that belong to the tertiary list in Eq. 28 and analyze solvabilities and hit ratios observed and predicted for the two solvers.

Results from first set are shown in Figure 12, which itself consists of *six subfigures*. The average values of *cntProbe* required by each solver to reach the best-known upper bound, are shown in Figures 12a and 12b. We can conclude by inspection that the solver `lssOrel_8` dominates `lssMAts` in terms of *cntProbe*. Notably, for $L > 107$, the gap in average values of *cntProbe* between `lssOrel_8` and `lssMAts` is statistically significant and also continues to increase with increasing value of L.

In Figure 12c we also observe a statistically significant and increasing gap in average values of *runtime* between the two solvers. However, in Figure 12d the observed speed of `lssOrel_8` is below the observed speed of `lssMAts` – with the gap slowly reducing as L increases. Apparently, solver `lssOrel_8` overcomes its speed disadvantage by significantly better *cntProbe* performance. For example, in the case of $L = 109$, the difference between mean values of *runtime* is 74 seconds and for $L = 127$, this difference increases to 1555 seconds. In conclusion, the solver of choice for the remainder of this paper is `lssOrel_8`, we settle on its mean runtime model (in unit of seconds) as

$$\overline{m}(L) = 0.000032 * 1.1504^L \tag{31}$$

A meticulous reader may notice that performance differences between the two solvers can also be attributed to differences in walk length segments between random restarts. By default, the solver `lssMAts` selects the walk segment length ω_{lmt} randomly from the interval $[\frac{L}{2}, \frac{3L}{2}]$

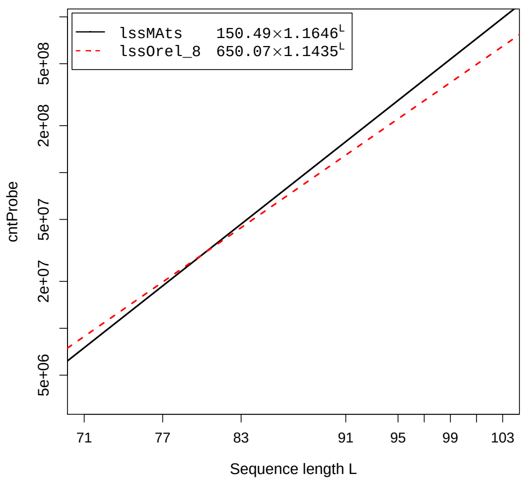

(a) *cntProbe* for $L = 71$ up to $L = 105$.

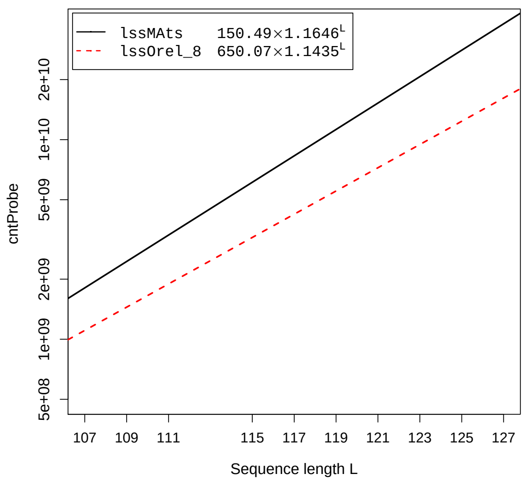

(b) *cntProbe* for $L = 107$ up to $L = 127$.

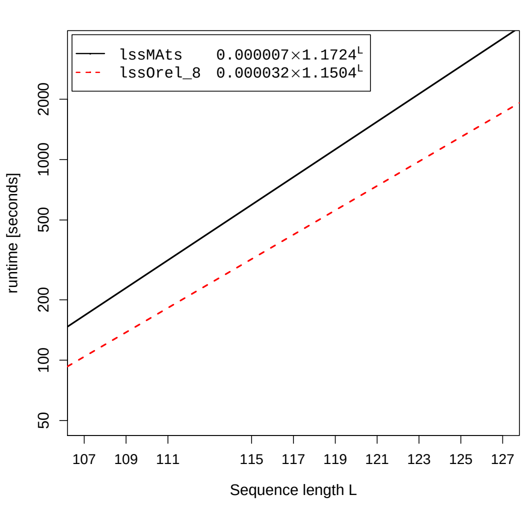

(c) *runtime* in seconds for $L = 107$ up to $L = 127$.

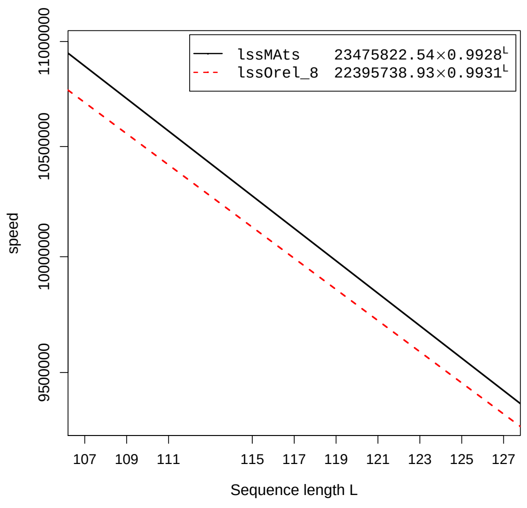

(d) *speed* for $L = 107$ up to $L = 127$.

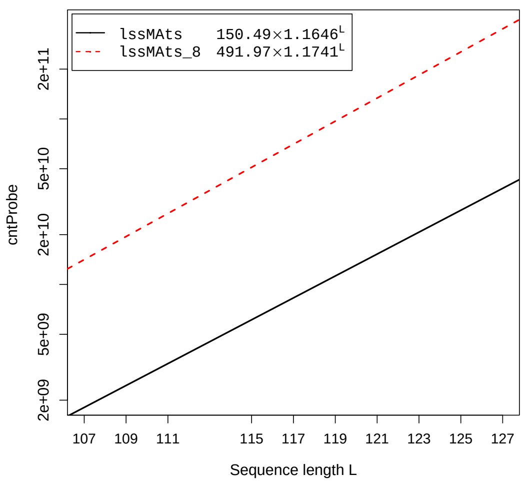

(e) `lssMAts` versus `lssMAts_8` only.

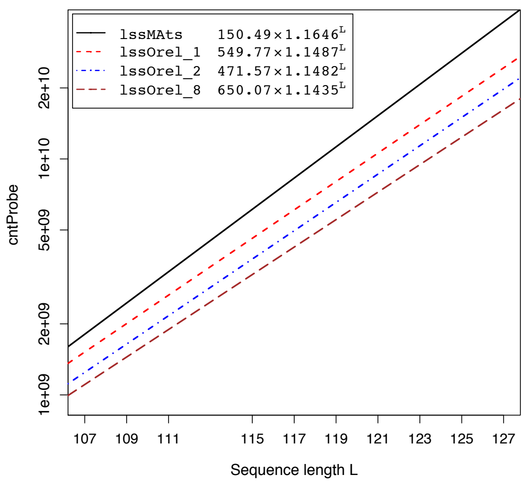

(f) `lssMAts` versus `lssOrel_8` and others.

Figure 12: Asymptotic average-case performance comparison between two solvers: `lssOrel_8` and `lssMAts`. While `lssMAts` dominates `lssOrel_8` in terms of *speed* performance, `lssOrel_8` exhibits a significantly better *cntProbe* performance which results in a significantly better *runtime* performance.

whereas for lssMAts_8 and lssOrel_8 we keep the walk segment length constant at $\omega_{lmt} = 8 * \frac{L+1}{2}$.

In Figure 12e, we compare the performance of lssMAts and lssMAts_8: the solver based on tabu search that extends the walk segment length to $\omega_{lmt} = 8 * \frac{L+1}{2}$ is at a significant disadvantage.

In Figure 12f, we compare lssMAts with lssOrel for values $\omega_c = 1, 2, 8$. We observe significant differences between lssMAts and all version of lssOrel. Even the version of lssOrel_1 with $\omega_{lmt} = \frac{L+1}{2}$, performs better than lssMAts, where on the average, ω_{lmt} is larger than $\frac{L+1}{2}$. In conclusion, we keep lssMAts as the default solver based on tabu search and lssOrel_8 as the default solver based on self-avoiding walk segments.

Results from the second set of experiments, based on seven instances from the tertiary list in Eq. 28, are shown in Table 5. Here we compare asymptotic predictions for *cntProbe*, calculated under the first set of experiments in Figure 12 versus the observed mean and observed solvability (defined as the sum of total of *cntProbe*, exhibiting a gamma distribution). There are a number of important observations that can be inferred from this set of experiments: (1) as long as the hit ratio stays at 100% (for all instance sizes up to L=141), the value differences between the model mean and the observed mean (and the asymptotic solvability and the observed solvability) are relatively small for *both* solvers, the differences increases significantly as the hit ratio reduces to 6% and 1% respectively; (2) for each instance, the asymptotic predictions represent the upper bound on the observed values (in this set of experiments); (3) for each instance, lssOrel_8 significantly outperforms lssMAts.

(8) Comparisons with best known merit factors. The new best-known merit factors returned by lssOrel_8 for all tertiary group instances that are greater than 160 and their *canonic solution* coordinates are shown in Table 6. For brevity, we list coordinates to represent *the first* $\frac{L+1}{2}$ binary symbols in the run-length notation. For example, the solution coordinate for L = 221 is listed as 7,11,1,2,2,... The value of 7 implies a run of seven 0's, followed by a run of eleven 1's, etc. Note these solutions are in the canonic form: each solution begins with a run of at least two 0's.

For additional empirical views that illustrate a number of the characteristics of the lssOrel_8, see Figure 13. In Figure 13a, we observe the quality of runtime predictions in comparisons with the observed lssOrel_8 runtimes. In Figure 13b, we use a large instance of $L = 241$ to demonstrate the variability in the quality of solutions reported by lssOrel_8: the runtime scatter plot and the histogram of best merit factors based on the sample size of 100. In this experiment, the only stopping criterion is the lssOrel_8 runtime limit of 4 days. The best-known merit factor for $L = 241$ has been 7.2747 [19]; represented with the blue line in the histogram. Observations of most interest in this figure include: (1) the point in the scatter graph on the extreme left, where the merit factor of 7.2 is reached near the very start of the experiment and *is not improved in 4 days*, and (2) the point on the extreme right, where the new best-known merit factor of 8.0668 is reached just before the end of the 4 day experiment. Overall, lssOrel_8 found 69 solutions with a merit factor better than 7.2747. Furthermore, the histogram shows that with the sample size of 100, there is only 1 solution with the best merit factor of 8.0668, and that there are now a total of 24 unique merit factor values that exceed the value 7.2747, currently reported as the best known value [19]. More computational resources, better solvers, or both are required to reach solutions with merit factor that will most likely exceed the value of 8.0668 for $L = 241$.

(9) Challenges for the next generation of labs solvers. We conclude the section with Figures 14 and 15. Both of these figures summarize the most important findings in this paper as well as the challenges for the next generation of labs solvers.

The table in Figure 14a compares merit factors obtained with lssOrel_8 with the best-known merit factors reported in the literature. Notably, lssOrel_8 always finds a solution that has equal or better merit factor than those reported earlier. The merit factors where the best-known solutions were not skew-symmetric are marked with *. All these solutions have been improved by lssOrel_8 and *all the best-known solutions for odd instance sizes greater than 100 are now skew-symmetric.* This is not unexpected; skew-symmetry significantly reduces the problem size and the solver has a better chance of finding new and better solutions for larger instances.

The table also lists additional columns: the observed number of hits *hitO* as defined in Eq. 10, the cardinality of the canonic solutions C_L as defined in Section 2, and the energy level difference $\Delta(E)$ of the improved solution with respect to the best-known previous solution. The value of $\Delta(E)$ conveys the significance of a given merit factor improvement. For example, for $L = 221$, the solver lssOrel_8 reports the merit factor of 8.8544 which represents a reduction of 448 energy level (under the constraint of skew-symmetry) with respect to the merit factor of 7.6171 reported by Knauer [19] (without the constraint of skew-symmetry). It is instructive to observe how the observed number of hits *hitO* relates to the the cardinality of canonic solutions C_L: $C_L \leq 2$ and remains as $C_L = 1$ for most of instances where $hitO > 1$, even when $hitO \gg 1$.

As the size of the labs problem increases, the monotonically decreasing number of observed hits *hitO* illustrates not only the limitation of lssOrel_8 it also suggests the need for massively parallel computational resources so that we can continue to maintain the observable hit ratio at 100% with $N \geq 100$. We argue that pursuing this strategy, we have the best chance of finding solutions with merit factors approaching the postulated limit of 12.3248.

The table in Figure 14b shows that the computational complexity of the new branch-and-bound solver [20],

Table 5: Predictions versus observations from experiments with `lssOrel_8` and `lssMAts`, under the constraint of runtime limit of 4 days for each of the selected values of L. The observed mean represents the sample mean based on the value of observed solvability (the sum total of *cntProbe* of each instance exhibits a gamma distribution). The observed hitRatio value of 100% signifies that none of the solutions have been censored. The model mean values are computed from the two predictors based on empirical data described in Figure 12. The values of predicted solvability, computed from Eq. 20, represent the value of *cntProbe* to reach hitRatio of 100% with probability of 0.99 – provided (1) the solver has been scheduled on a single CPU invoke on each instance serially, and (2) the solution produced by the solver has not been censored.

	`lssOrel_8`					`lssMAts`				
L	model mean*	observed mean	predicted solvability†	observed solvability	*solvP*‡	model mean+	observed mean	predicted solvability†	observed solvability	*solvP*‡
115	3.236e+09	2.858e+09	4.037e+11	2.858e+11	100	6.135e+09	6.132e+09	7.652e+11	6.131e+11	100
121	7.236e+09	6.539e+09	9.025e+11	6.539e+11	100	1.530e+10	1.335e+10	1.909e+12	1.334e+12	100
127	1.617e+10	1.479e+10	2.017e+12	1.479e+12	100	3.819e+10	2.997e+10	4.763e+12	2.997e+12	100
141	1.057e+11	5.339e+10	1.318e+13	5.339e+12	100	3.224e+11	1.611e+11	4.021e+13	1.610e+13	100
151	4.042e+11	3.874e+11	5.041e+13	3.874e+13	95	1.479e+12	7.363e+11	1.845e+14	7.363e+13	80
161	1.545e+12	7.033e+11	1.927e+14	7.033e+13	76	6.791e+12	1.200e+12	8.470e+14	1.200e+14	44
181	2.257e+13	1.221e+12	2.816e+15	1.221e+14	6	1.430e+14	1.338e+12	1.784e+16	1.338e+14	1
	*cntProbe(`lssOrel_8`) $= 650.07 * 1.1435^L$					+cntProbe(`lssMAts`) $= 150.49 * 1.1646^L$				

† using Eq. 20 with $N = 100, p = 0.99$; ‡ using Eq. 10

Table 6: New best-known solutions provided by `lssOrel_8`. Solution coordinates of length $\frac{L+1}{2}$ are shown in run length encoded notation. Rules of skew-symmetry must be applied to expand each cooodinate to its full length L.

L	F	E	solution coordinate (in canonic form, e.g. for $L = 181$, 11 represents a run of eleven 0's)
181	8.9316	1834	11,1,2,1,4,4,2,3,2,1,1,3,2,2,2,1,2,2,1,2,3,4,1,2,1,1,4,1,2,1,1,2,3,1,1,6,1,1,4,1,1
201	8.4876	2380	9,1,2,2,1,2,1,2,1,6,8,2,1,6,1,1,2,1,2,5,1,1,1,2,1,2,1,1,3,3,5,1,1,2,6,2,3,2,2,2,2,1
215	8.5888	2691	4,3,1,1,3,4,1,1,1,1,1,4,1,1,1,1,1,2,1,2,2,1,2,1,1,2,5,1,2,1,3,3,2,2,1,3,1,1,1,4,2,2,1,4,1,1,2,2,1,3,1,1,1,1,4,4,3
221	8.8544	2758	7,11,1,2,2,1,2,1,2,2,1,2,6,6,1,1,2,1,2,1,2,1,4,1,1,1,2,1,7,2,2,1,3,2,1,2,1,2,1,2,1,1,4,3,1,1,2,2,3
241	8.0668	3600	2,1,1,2,1,2,2,1,1,1,1,3,1,2,1,5,1,2,1,5,1,1,2,2,3,2,1,3,5,2,1,5,1,4,1,1,2,3,1,2,4,1,4,3,2,1,3,1,1,2,1,3,1,1,3,2,1,2,1,1,1,1,1,1
249	8.1323	3812	4,1,2,1,2,1,1,2,2,1,4,1,2,1,4,1,3,6,2,1,4,1,2,7,3,1,2,1,2,1,2,5,2,1,2,1,2,1,12,1,3,5,1,1,1,4,1,2,3,1,1,2,1,2,2
259	8.0918	4145	3,3,1,3,2,3,2,1,4,1,3,5,4,1,4,1,1,1,1,2,1,4,2,3,3,3,3,2,1,1,1,1,2,3,2,6,3,1,1,4,1,2,2,1,3,4,1,2,1,5,1,5,1,3,1,1,1,2
261	7.8517	4338	2,2,2,1,1,1,1,2,1,1,1,4,1,2,1,2,1,1,4,1,1,1,3,2,2,1,1,1,1,1,2,2,1,3,1,2,1,4,1,1,1,1,1,2,3,1,1,1,2,1,1,2,3,1,1,1,2,2,1,5,1,1,1,2,1,1,2, 1,2,2,1,1,1,8,2,2,3,2
271	7.5386	4871	3,3,1,1,1,1,3,1,1,4,2,1,3,3,2,1,1,1,1,1,1,1,1,2,3,2,3,1,3,3,2,1,1,1,2,4,4,1,2,4,4,1,1,1,1,2,2,1,1,1,2,1,2,1,1,3,1,4,3,2,3,1,1,1,1,1,3, 6,1,2,2,2
281	7.5058	5260	15,3,3,10,2,3,2,2,1,4,2,3,2,2,3,2,1,4,4,2,1,5,3,2,4,1,1,1,2,3,2,4,2,1,3,3,1,1,7,2,1,3,2,1,1,1,1,1,2,1,1,1,2,1,2,1
283	7.5088	5333	4,1,1,11,1,1,1,1,9,1,3,3,1,2,1,2,1,1,1,2,2,3,2,4,1,1,1,1,2,1,3,2,2,2,1,1,2,1,1,1,4,2,3,3,2,2,5,3,1,2,1,3,2,1,1,2,1,1,3,2,1,2,1,1,1,1, 2,1,2,1,1,2
301	7.4827	6054	3,3,3,3,3,3,4,2,3,5,1,1,2,5,3,1,2,1,1,1,1,1,1,2,1,3,1,3,2,3,6,1,1,1,1,1,2,3,2,7,6,2,1,1,1,1,3,3,1,3,1,1,1,1,1,3,1,2,1,3,1,2,2,1,1,1,1, 1,1,2,1,2,2,2,1
303	7.2462	6335	2,1,1,2,2,1,2,2,2,1,1,1,1,1,1,1,1,2,1,1,2,2,1,1,1,1,1,1,1,2,1,2,1,2,2,2,3,1,1,1,1,1,2,3,1,1,2,1,1,1,4,1,2,1,2,2,2,1,1,1,1,1,1,2,1,2,3, 2,2,1,1,1,1,4,1,1,1,2,1,1,1,1,2,2,1,6,2,1,1,3,3,1,1,1,4,2,1,1,1
341	6.9397	8378	2,4,3,1,1,2,2,2,1,2,1,2,1,3,1,2,2,1,6,5,2,2,1,1,3,1,3,3,1,1,1,4,3,2,1,1,2,1,1,3,1,2,1,1,1,1,1,1,5,5,1,2,1,2,4,1,1,3,5,1,1,1,1,3,1,1,1, 4,1,1,2,3,1,1,3,3,1,2,1,3,2,4,1,1,1,1,1,1,2,1,1
381	7.0893	10238	5,2,1,2,1,6,2,1,7,2,2,2,1,2,2,1,2,1,2,1,2,1,2,2,2,2,1,7,6,2,1,2,6,2,1,2,5,5,2,1,7,4,9,1,1,2,2,3,6,1,1,2,1,2,1,1,2,1,2,2,5,1,1,1,5,1,2, 1,3,1,3,1,1,7,1,1,1,4,1
401	6.7632	11888	2,4,1,2,4,1,5,1,1,2,1,2,1,1,2,5,6,2,4,5,1,1,2,3,2,2,4,1,2,3,1,4,1,2,3,4,1,3,2,1,2,1,1,1,3,2,1,1,1,2,3,4,3,1,5,2,1,4,2,5,1,1,1,1,1,1,1, 1,1,1,2,3,1,2,1,3,2,2,2,3,1,6,1,1,1,1,1,1,5,1,1,1,2,1,2,1,3

now limited to odd values of L under skew-symmetry, is $O(1.3370^L)$. However, the B&B solver scales poorly and the stochastic solvers are the only viable alternative. Both `lssMAts` and `lssOrel_8` stochastic solvers can find the same optimum solutions with significantly less computational effort, even when comparing a single run with the branch and bound solver with the runtime for 100 repeated runs of each stochastic solver.

The hit ratio model $hitP_r$ in Figure 14c predicts, for the solver `lssOrel_8`, the probability of reaching *uncensored valueBest = valueTarget* solutions on a grid of N independent processors, given (1) the runtime limit in days of $t_{lmt} \in (4, 8, 16, ..., 128)$, (2) the ideal value of processor load factor $loadFactor = 1$, and (3) $\overline{m}(L) = 0.000032 * 1.1504^L/(3600 * 24))$. The agreement with the predicted number of hits, *hitP*, versus the observed number of hits, *hitO* in the small table summary under empirically determined $loadFactor = 2.4$ under [46] is as remarkable as is the agreement with the mean value runtime predictions versus the observed runtime means for the solver `lssOrel_8` and values of $L \leq 141$, i.e. the table shown in Figure 13a.

In Figure 15 we contrast two views of merit factor asymptotics as L increases towards the value of 5000. In Figure 15a, the merit factors rely on Legendre sequences, using a construction technique similar to [33, 34]. A few short and mostly very long sequences, and with merit factors hovering around 6.34, can be computed in polynomial runtime $O(L^3)$. The best merit factor under this construction, 6.40667, has been found for $L = 31$. On the other hand, as shown in Figure 15b, all merit factors found by `lssOrel_8` are well above 6.34, some with merit factors larger than 9.0, and all below 10.0. In Figure 7 we show that even to find the binary sequence of length $L = 573$ with merit factor of at least 6.34, the average runtime for the current generation of stochastic solvers such as

(a) Mean value runtime predictions versus the observed runtime means with the solver `lssOrel_8`: $\overline{m}(L) = 0.000032*1.1504^L$ (Eq. 31) versus $\overline{m}_{obs}(L)$. For values of $L \leq 141$, none of the $N = 100$ runs are censored within the time limit of $t_{lmt} = 4$ days (345600 seconds), hence the observed number of hits is *hitO = 100* and the reported values of observed runtime means are within the confidence interval defined in Eq. 15. Relative to the predicted value of $\overline{m}(L)$, the ratio of $\overline{m}_{obs}(L)/\overline{m}(L) > 1$ is an indicator of the instance solvability as well as the level of the landscape frustration [51]; a characteristic of the the `labs` problem. All instances with more than a single canonic solution ($C_L > 1$) have been excluded from this prediction model. For $L = 141$, $C_{141} = 2$.

L	$\overline{m}(L)$	$\overline{m}_{obs}(L)$	Δ(seconds)	ratio	C_L
83	3	12	9	4.00	1
91	11	7	-4	-0.63	1
95	19	30	11	1.58	1
97	25	28	3	1.12	1
99	33	14	-19	-0.42	1
101	44	34	-10	-0.77	1
103	59	48	-11	-0.81	1
105	78	69	-9	-0.88	1
107	103	446	343	4.33	1
109	137	83	-54	-0.61	1
111	181	154	-27	-0.85	1
115	318	279	-39	-0.87	1
117	421	299	-122	-0.71	1
119	557	355	-202	-0.63	1
121	737	673	-64	-0.91	1
123	976	2181	1205	2.23	1
125	1291	1427	136	1.11	1
127	1709	1598	-111	-0.94	1

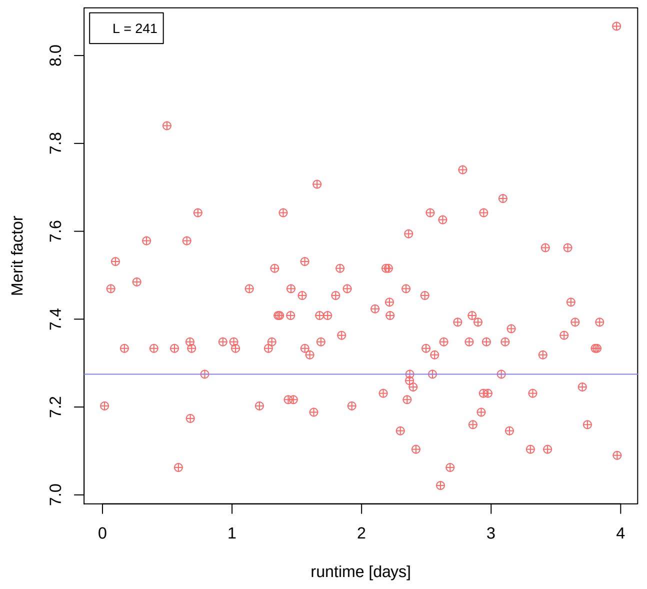

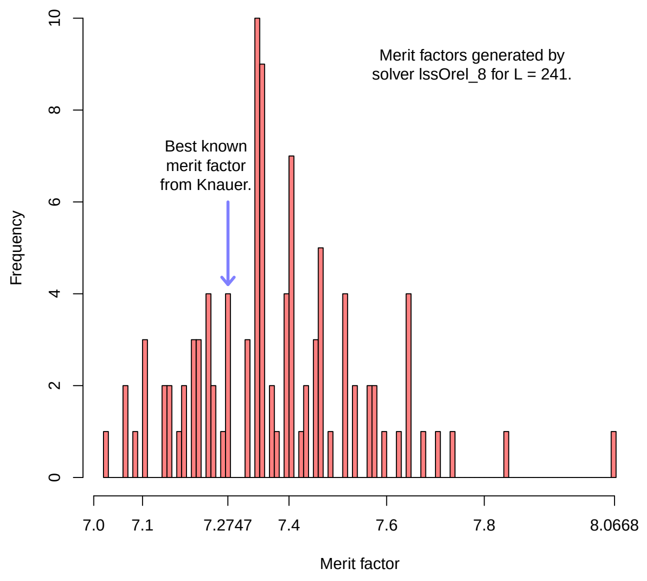

(b) $L = 241$: a runtime scatter plot of best merit factors and a histogram of merit factor frequencies

Figure 13: Two empirical views illustrating the `labs` problem: (a) the asymptotic runtime predictions and observations, (b) best merit factors for $L = 241$ in a special-case experiment with `lssOrel_8` running on 100 instances for a total of 4 days.

`lssOrel_8` is around 32 years. Nevertheless, the trend of merit factors achieved with `lssOrel_8` in Figure 15b points in the right direction – as long as we continue to find *uncensored solutions* with progressively increasing merit factors. Currently, sequences that would converge closer to the conjectured asymptotic value of 12.3248 are yet to be discovered. In order to find better merit factors as L increases we need both: new approaches to design better solvers and a significant increase in computational resources.

5. Discussion

This paper focuses on the stochastic solvers for the `labs` problem. Stochastic solvers can not guarantee optimal solutions. We can compare the performance of each solver only by measuring the memory footprint, the walk length, the probe count, and the runtime until it returns a solution coordinate with *the best known value* (*BKV*) – which may or may not be an optimum value. When *BKV* is not improved, only repeated after a large number of independent experiments, a statistician can make not only a *reliable* statement about the average-case performance of the specific solver but also about the probability of ever finding a better solution with the given solver.

The branch-and-bound solvers do guarantee optimal solutions, but only for instance of size up to $L = 66$ without the use of skew-symmetry and up to $L = 119$ [12] with the use of skew-symmetry. In contrast, the new stochastic solver `lssOrel`, also using skew-symmetry, returned solutions with *BKVs* that match *all* of the exact solutions

L	[5]	[3]	[22]	[27]	[24]	[50]	[29]	[30]	lssOrel_8	*hitO*	C_L	$\Delta(E)$
107	6.53	**8.46**	**8.46**	8.36	**8.46**	**8.4557**	-	**8.4557**	**8.4557**	100	1	0
109	6.15	**8.97**	**8.97**	**8.97**	**8.97**	**8.9736**	-	**8.9736**	**8.9736**	100	1	0
111	6.02	**8.97**	**8.97**	**8.97**	**8.97**	**8.9672**	-	**8.9672**	**8.9672**	100	1	0
113	6.33	**8.49**	**8.49**	**8.49**	**8.49**	**8.4900**	-	**8.4900**	**8.4900**	100	2	0
115	6.40	**8.88**	8.60	**8.88**	**8.88**	**8.8758**	-	**8.8758**	**8.8758**	100	1	0
117	6.42	**8.71**	8.12	**8.71**	**8.71**	**8.7080**	-	**8.7080**	**8.7080**	100	1	0
119	6.01	-	7.67	**8.48**	8.02	**8.4796**	-	**8.4796**	**8.4796**	100	1	0
121	6.61	-	**8.67**	-	**8.67**	**8.6736**	-	**8.6736**	**8.6736**	100	1	0
141	6.01	-	7.45	-	**8.83**	**8.8282**	-	**8.8282**	**8.8282**	100	2	0
149	-	-	-	-	-	**9.1137**	**9.1137**	-	**9.1137**	95	1	0
157	-	-	-	-	-	**9.0223**	**9.0223**	-	**9.0223**	98	1	0
161	6.02	-	6.89	-	8.39	8.5266	-	**8.5718**	**8.5718**	76	2	0
165	-	-	-	-	-	**9.2351**	**9.2351**	-	**9.2351**	26	1	0
169	-	-	-	-	-	**9.3215**	**9.3215**	-	**9.3215**	24	1	0
173	-	-	-	-	-	9.3179	**9.3645**	-	**9.3645**	28	1	0
175	-	-	-	-	-	8.9078	**9.0768**	-	**9.0768**	12	1	0
177	-	-	-	-	-	8.6640	**9.5052**	-	**9.5052**	10	1	0
179	-	-	-	-	-	8.4452	**9.0974**	-	**9.0974**	6	1	0
181	7.70	-	6.77	-	7.75	8.6304	-	7.7194	**8.9316**	6	1	64
183	-	-	-	-	-	8.3932	**9.0073**	-	**9.0073**	5	2	0
189	-	-	-	-	-	**9.0847**	**9.0847**	-	**9.0847**	1	1	0
201	-	-	6.29	-	7.46	8.2116	-	7.6633	**8.4876**	1	1	80
215	-	-	-	-	-	8.1641*	-	-	**8.5888**	1	1	140
221	-	-	-	-	-	7.6171	-	-	**8.8544**	1	1	448
241	-	-	-	-	-	7.2747	-	-	**8.0668**	1	1	392
249	-	-	-	-	-	7.2431*	-	-	**8.1323**	1	1	468
259	-	-	-	-	-	7.1287*	-	-	**8.0918**	1	1	560
261	-	-	-	-	-	7.1108*	-	-	**7.8517**	1	1	452
271	-	-	-	-	-	7.0037*	-	-	**7.5386**	1	1	372
281	-	-	-	-	-	7.0957	-	-	**7.5058**	1	1	304
283	-	-	-	-	-	7.0291*	-	-	**7.5088**	1	1	364
301	-	-	-	-	-	-	-	-	**7.4827**	1	1	-
303	-	-	-	-	-	7.1115	-	-	**7.2462**	1	1	120
341	-	-	-	-	-	-	-	-	**6.9397**	1	1	-
381	-	-	-	-	-	-	-	-	**7.0893**	1	1	-
401	-	-	-	-	-	-	-	-	**6.7632**	1	1	-

(a)

L	runtime [years]		100 × runtime [years]	
	BB	ratio†	lssOrel_8	lssMAts
75	1.1590e-04	3.1194e+03	3.7154e-06*	3.3649e-06^{+}
77	2.8983e-04	5.7999e+03	4.9971e-06	4.7695e-06
79	5.6726e-04	8.7172e+03	6.5074e-06*	6.3574e-06^{+}
81	8.9805e-04	1.0428e+04	8.6120e-06*	8.7384e-06^{+}
83	1.1310e-03	2.8420e+03	3.9795e-05	8.5217e-06
85	2.3780e-03	1.5766e+04	1.5083e-05*	1.6510e-05^{+}
87	4.5392e-03	2.2739e+04	1.9962e-05*	2.2693e-05^{+}
89	9.0476e-03	3.4249e+04	5.3345e-06	1.0364e-05
115	1.5758e+01*	1.7756e+06	8.8751e-04	1.8324e-03
121	9.0011e+01*	4.2144e+06	2.1358e-03	4.2444e-03
127	5.1414e+02*	1.0145e+07	5.0680e-03	1.0521e-02
141	2.9986e+04*	7.7784e+07	3.8551e-02	1.2189e-01
151	5.4732e+05*	3.4972e+08	1.5650e-01*	5.9805e-01^{+}
161	9.9897e+06*	1.5723e+09	6.3534e-01*	2.9342e+00^{+}
181	3.3280e+09*	3.1783e+10	1.0471e+01*	7.0634e+01^{+}
201	1.1087e+12*	6.4245e+11	1.7257e+02*	1.7003e+03^{+}
241	1.2304e+17*	2.6322e+14	4.6744e+04*	9.8259e+05^{+}

The unmarked values have been observed experimentally,
the values marked with * and $^{+}$ are based on predictions below:
BB = 1.55311e-06*$1.3370^L/(3600*24*366)$
† ratio = runtime(BB)/runtime(lssOrel_8)
* lssOrel_8 = $100*(0.000032*1.1504^L/(3600*24*366))$
$^{+}$ lssMAts $= 100*(0.000007*1.1724^L/(3600*24*366))$

(b)

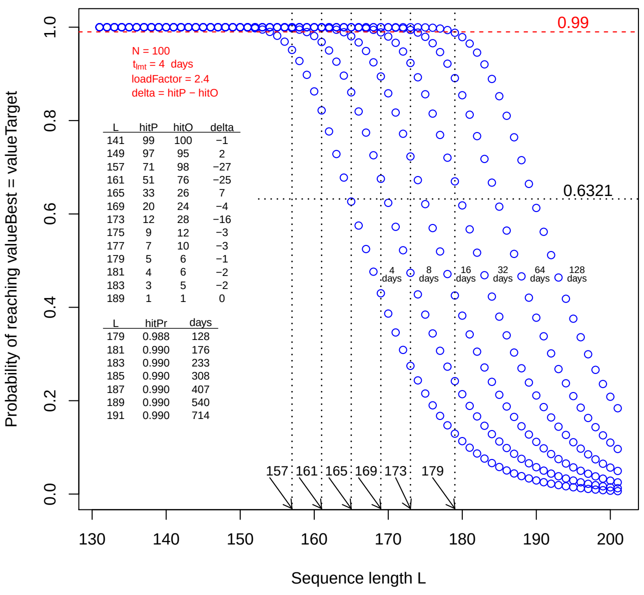

L	hitP	hitO	delta
141	99	100	−1
149	97	95	2
157	71	98	−27
161	51	76	−25
165	33	26	7
169	20	24	−4
173	12	28	−16
175	9	12	−3
177	7	10	−3
179	5	6	−1
181	4	6	−2
183	3	5	−2
189	1	1	0

L	hitPr	days
179	0.988	128
181	0.990	176
183	0.990	233
185	0.990	308
187	0.990	407
189	0.990	540
191	0.990	714

(c)

Figure 14: (a) Comparisons of the best-known merit factors reported in the literature and the best-known merit factors obtained by lssOrel_8. (b) Observed/predicted asymptotic performance of state-of-the-art branch-and-bound labs solver under skew-symmetry [20] versus the observed/predicted runtime of two stochastic solvers under skew-symmetry: lssOrel_8 and lssMAts. (c) A hit ratio model $hitP_r$ for the solver lssOrel_8 predicts the probability of reaching *uncensored valueBest* = *valueTarget* solutions on a grid of N independent processors, given (1) the runtime limit in days of $t_{lmt} \in (4, 8, 16, ..., 128)$, (2) the ideal value of processor load factor $loadFactor = 1$, and (3) $\overline{m}(L) = 0.000032 * 1.1504^L/(3600 * 24)$. In other words, when $hitP_r \geq 0.99$, we predict that at most 1% of the N instances may be censored by the solver. The table summary under the headline of $loadFactor = 2.4$ displays a remarkable agreement with the predicted number of hits ($hitP$) versus the observed number of hits ($hitO$); the empirical value of $loadFactor = 2.4$ is associated with [46]. Small deviations in the column **delta** are of the same order as the ones explained in Figure 13-a. For formulas about $hitO$, $hitP$, $hitP_r$, and $\overline{m}(L)$ see Eqs. 10, 16, 17, 31.

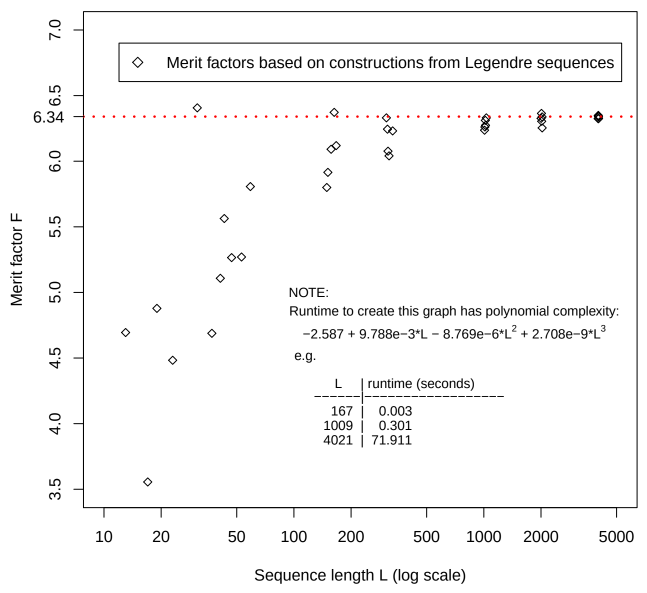

(a) merit factors based on constructions from Legendre sequences

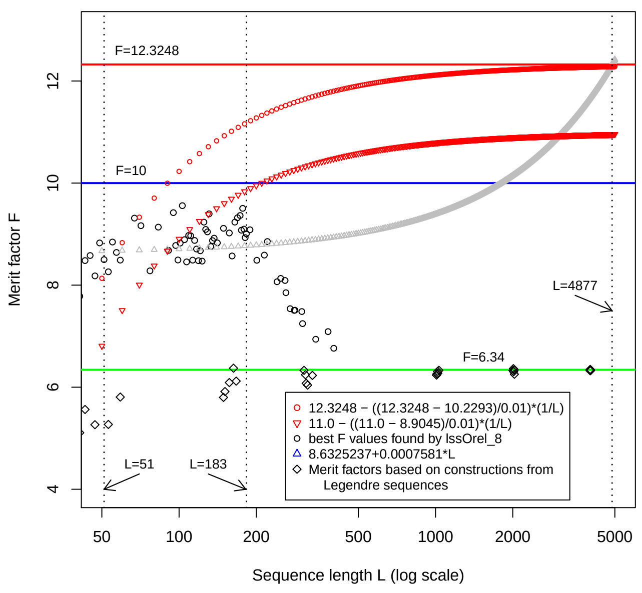

(b) asymptotes and merit factors based a stochastic solver

Figure 15: We contrast two views of merit factor asymptotics as L increases towards the value of 5000. In (a), the merit factor values are based on constructions from Legendre sequences, using a technique similar to [33, 34]. Parameters r and t are taken in increments of $1/L$: for $L < 500$, $r \in [0, 0.5], t \in [0, 0.1]$; for $L \geq 500$, $r \in [0.2, 0.24], t \in [0.055, 0.063]$. Notably, the observed merit factor variability is decreasing rapidly as L increases. For the prime values of (13, 17, 19, 23, 31, 37, 41, 43, 47, 53, 59), values of F range from 3.55556 to 6.40667. For the prime values of (149, 151, 157, 163, 167), values of F range from 5.79981 to 6.37224. For the prime values of (1009, 1013, 1019, 1021, 1031), values of F range from 6.23938 to 6.33041 and runtime for each value of L is less than 1 CPU second. For the prime values of (4003, 4007, 4013, 4019, 4021), values of F range from 6.32348 to 6.34917 and runtime for each value of L is $\approx$ 72 CPU seconds. The runtime complexity to construct these sequences is $O(L^3)$. In (b), the linear model $8.6325237 + 0.0007571 * L$ 'predicts' to cross the conjectured asymptotic value of 12.3248 at $L = 4877$. This model is based on extrapolation of *observed merit factor values* in Figure 1d: for $L > 50$ and $L \leq 183$, the values of F range from 8.2618 to 9.5577. The crossover value of $L = 4877$ may at this point be pessimistic. On the other hand, there is a rigorous interpretation for the slope provided by Bernasconi in Figure 1b, see Figure 5 and Equations 22-24 in [7]. By interpreting the slope at 12.3248 in Figure 1b as (12.3248 - 10.2293)/0.01), we create a non-linear predictor $b_U = 12.3248 - ((12.3248 - 10.2293)/0.01) * (1/L)$ as an upper bound and $b_L = 11.0 - ((11.0 - 8.9045)/0.01) * (1/L)$ as its lower bound counterpart. For a reality check, recall the runtime asymptotics for the better of the two solvers, `lssOrel_8`, extrapolated from Figure 11c: $0.000032 * 1.1504^L$ (Eq. 31), implying the mean runtime to solve for 'the best merit factor' for $L = 161$ approaches 2.32 days (on a single CPU) and is increasing rapidly: 28.9 days for $L = 179$, 629.9 days for $L = 201$, and 467 years for $L = 241$.

reported by branch-and-bound solvers – not only in a single experiment and in a small fraction of runtime required by the branch-and-bound solver, but also in at least 100 independent experiments. Moreover, `lssOrel` now reports *BKVs* for skew-symmetric instances $119 < L \leq 401$ on a grid of 100 processors with a runtime limit of 4 days. The number of repeated *BKVs* drops from 100 to 95, 76, 6, 1 starting with instances $L \geq 151$.

The analysis of the self-avoiding walk reveals that on smaller instances the solver `lssOrel_U`, where the length of the walk segment is kept at 'unlimited', has an advantage over the nominal solver where the walk segment length is limited. However, as L increases, the advantage of `lssOrel_U` decreases in terms of *runtime*. The reason for the reduced efficiency of the solver is the *runtime* cost of memory management, necessary to maintain the self-avoiding walk. The instance with $L = 105$ hits the memory restriction of 8 GB on our processor. The experiments show that with `lssOrel_8`, where the length of the walk segment is limited to $8 * \frac{L+1}{2}$, we get the best asymptotic average case performance: cntProbe is $650.07 * 1.1435^L$ and the memory footprint is constant at about 1.8 MB.

The rigorous asymptotic experiments with solvers `lssMAts` and `lssRRts`, both using the tabu search, show that (1) the evolutionary component within `lssMAts` is not effective and (2), the solver `lssOrel_8` significantly outperform `lssMAts`. The same asymptotic performance testing methodology, including the platform-independent performance comparisons, can be applied to engineering the next generation of `labs` solvers.

6. Conclusions And Future Work

This paper introduces a new stochastic solver and demonstrates its merits by following a rigorous methodology of experimental design. We now have models that predict not only the asymptotic runtime performance of this solver, we also have similar models for alternative state-of-the-art solvers [30]. Moreover, we have shown why the new *self-avoiding walk search* solver `lssOrel` dominates the solver `lssMAts` (memetic/tabu search) and why the solvers `lssRRts` (tabu search only) and `lssMAts` are equivalent – at least when applied to the `labs` problem. Despite their superficial similarities, the self-avoiding walk search and

Table 7: Predictions, based on Eq. 18, for the required number of processors N running concurrently for 5 years (5*365 days) in order to get at least 100 repeated hits of the best known merit factor with the solver lssOrel_8. In this table, the runtime for each processor is reported in days:
$runtime(\texttt{lssOrel\_8}) = (0.000032 * 1.1504^L)/(3600 * 24)$

L	*runtime*	N
199	4.759e+02	1.030e+02
216	5.152e+03	3.360e+02
246	3.447e+05	1.893e+04
283	6.149e+07	3.369e+06
333	6.781e+10	3.715e+09

the long-established tabu search are not equivalent.

We borrowed the notion of self-avoiding walk from chemists and physicists. In the follow-up work, we are generalizing these stochastic walks – on directed vertex-weighted graphs – as being Hamiltonian as well as Eulerian [52]. For example, the Hamiltonian walk illustrated in Figure 2b reaches the target vertex in 17 steps. However, by considering edges as bidirectional and switching to an Eulerian walk after the step 7, we can reach the target vertex in 11 steps only. Work in progress includes an exploration of new walk strategies to improve the current `labs` solver; such strategies are also showing promising results in domains of other combinatorial problems, ranging from *optimum Golomb ruler* or `ogr` problem, minimum vertex/set cover, linear ordering, protein folding, and beyond. A version of the new walk strategies is particularly effective in solving the `ogr` problem [53]; the new solver already dominates a state-of-the-art memetic solver [54].

The invariants that characterize `lssOrel` are the models for the *average cntProbe*, *walkLength*, and *runtime*. These invariants are standards that should not only be met but also improved by the new `labs` solver. Both *cntProbe* and *walkLength* facilitate platform-independent performance comparisons with other solvers. Thus:

$$\begin{aligned} cntProbe(\texttt{lssOrel\_8}) &= 650.07 * 1.1435^L \qquad (32)\\ walkLength(\texttt{lssOrel\_8}) &= 35.51 * 1.1321^L\\ runtime(\texttt{lssOrel\_8}) &= 0.000032 * 1.1504^L \end{aligned}$$

For a bigger picture about the hardness of of the `labs` problem, we contrast it with the `ogr` problem, given that our experiments with `ogr` solvers in [53] show that the asymptotic runtime complexity of a stochastic `ogr` solver is significantly lower than the complexity of `lssOrel_8`. Consider the results in Table 7. We use the Eq. 18 to predict the required number of processors N running concurrently for 5 years (5*365 days) in order to get at least 100 repeated hits of the best known merit factor with the solver `lssOrel_8`. In the example that follows Eq. 18 we take $L = 179$, a runtime limit of 4 days (under the *loadFactor* of 2.4), find $hitP_r = 0.05607801$ and get the prediction of $N = 1784$ processors that we should run concurrently in order to achieve at least $N_c = 100$ hits (repeated best-known value solutions). In Table 7 we choose a runtime limit of 5 years (5*365 days with a *loadFactor* of 1) and assign a subset of values of L associated with the known optimum Golomb rulers. The choice of the runtime limit of 5 years is related to the *waiting time*, under *massively parallel computational effort*, that elapsed before finding the optimal ogr solution for $L = 553$ in 2014 [55, 56].

Given results in Table 7, finding the near-optimum values for the `labs` problem with $L > 246$ may not be an option unless we devise a faster solver. Revisiting the 100-processor, 4-day experiment with $L = 241$ in Figure 13, we find that under a runtime limit of 5 years we need to run in parallel at least 9425 processors. This number increases to 46923 processors if the runtime limit is 1 year.

In conclusion, the paper reports a number of important computational milestones. Using the grid environment with only 100 processors and a runtime limit of only 4 days, `lssOrel` either re-confirmed or improved the best merit factors reported in the literature. For some instances the improvement is huge. For $L = 259$, the best merit factor was improved from 7.1287 to 8.0918 which represents a reduction of 560 energy levels, from 4705 to 4145. All of the best known solutions for instances with $L_{odd} > 100$ are now skew-symmetric.

Acknowledgments

This work was supported in part by the Slovenian Research Agency under program P2-0041: Computer Systems, Methodologies, and Intelligent Services.

We gratefully acknowledge the cooperation of José E. Gallardo, Carlos Cotta and Antonio J. Fernández in providing the source code of solvers `lMAts` and `lssMAts`.

We also thank for the generous advice and encouragement offered by Dr. Jacob Bernasconi. The comments from anonymous reviewers helped to clarify a number of points in the paper. For the presentation of results, we were greatly influenced by the features offered in R [48] and the arguments in [57].

Source code release

For links to (1) comprehensive tables of *best-known-value solutions*, (2) the number of *unique* solutions in *canonic form* and the solutions themselves, (3) the source code of relevant solvers, and (4) the `xBed` statistical testing environment, customized for the `labs` problem, see [19].

In addition, a crowd-sourcing server prototype to facilitate experimentation and push the frontiers on finding new *best-known values, BKVs,* for the `labs` problem is under construction. Researchers will be able to download the `labs` solver `lssOrel_8` with the data set and simply *run the solver on their host* in the browser. Upon finding the solution (or a breakthrough value that improves the current *BKV*), the browser will return solution details to the server and start a new run on the local host either with the current or the new *BKV*. For an interactive `labs` puzzle and the timeline of the crowd-sourcing server prototype availability [19].

References

[1] M. J. Golay, Sieves for low autocorrelation binary sequences, IEEE Transactions on Information Theory 23 (1977) 43–51. doi:10.1109/TIT.1977.1055653.

[2] M. J. Golay, The merit factor of long low autocorrelation binary sequences, IEEE Transactions on Information Theory IT-28 (3) (1982) 543–549. doi:10.1109/TIT.1982.1056505.

[3] M. J. Golay, D. B. Harris, A new search for skewsymmetric binary sequences with optimal merit factors, IEEE Transactions on Information Theory 36 (5) (1990) 1163–1166. doi:10.1109/18.57219.

[4] M. Golay, A class of finite binary sequences with alternate autocorrelation values equal to zero, IEEE Trans. Inf. Theor. 18 (3) (1972) 449–450. doi:10.1109/TIT.1972.1054797.

[5] G. Beenker, T. Claasen, P. Hermens, Binary sequences with a maximally flat amplitude spectrum, Philips J. Res. vol. 40 (1985) 289–304.

[6] I. A. Pasha, P. S. Moharir, N. S. Rao, Bi-alphabetic pulse compression radar signal design, Sadhana 25 (5) (2000) 481–488. doi:10.1007/BF02703629.

[7] J. Bernasconi, Low autocorrelation binary sequences: statistical mechanics and configuration space analysis, J. Phys. 48 (1987) 559–567. doi:10.1051/jphys:01987004804055900.

[8] J. Littlewood, Some problems in real and complex analysis, Heath mathematical monographs, D. C. Heath, 1968.

[9] P. Borwein, Computational Excursions in Analysis and Number Theory, Springer-Verlag, 2002. doi:10.1007/978-0-387-21652-2.

[10] P. F. Stadler, Landscapes and their correlation functions, Journal of Mathematical Chemistry 20 (1) (1996) 1–45. doi:10.1007/BF01165154.

[11] K.-U. Schmidt, J. Willms, Barker sequences of odd length, Designs, Codes and Cryptography 80 (2) (2016) 409–414. doi:10.1007/s10623-015-0104-4.

[12] T. Packebusch, S. Mertens, Low autocorrelation binary sequences, Journal of Physics A: Mathematical and Theoretical 49 (16) (2016) 165001. doi:10.1088/1751-8113/49/16/165001.

[13] E. Marinari, G. Parisi, F. Ritort, Replica field theory for deterministic models: I. binary sequences with low autocorrelation, Journal of Physics A: Mathematical and General 27 (23) (1994) 7615–7645. doi:10.1088/0305-4470/27/23/010.

[14] J. Jedwab, A Survey of the Merit Factor Problem for Binary Sequences, in: T. Helleseth, D. Sarwate, H.-Y. Song, K. Yang (Eds.), Sequences and Their Applications - SETA 2004, Vol. 3486 of Lecture Notes in Computer Science, Springer Berlin Heidelberg, 2005, pp. 30–55. doi:10.1007/11423461_2.

[15] A. Ukil, Low autocorrelation binary sequences: Number theory-based analysis for minimum energy level, Barker codes, Digit. Signal Process. 20 (2) (2010) 483–495. doi:10.1016/j.dsp.2009.08.003.

[16] J. Bernasconi, personal communication (2015).

[17] M. Pelikan, D. E. Goldberg, HHierarchical BOA Solves Ising Spin Glasses and MAXSAT, in: Proceedings of the 2003 international conference on Genetic and evolutionary computation: PartII, GECCO'03, Springer-Verlag, Berlin, Heidelberg, 2003, pp. 1271–1282. doi:10.1007/3-540-45110-2_3.

[18] S. Mertens, Exhaustive search for low-autocorrelation binary sequences, Journal of Physics A: Mathematical and General 29 (1996) 473–481, The sequences for $48 < L \leq 60$ have been found with an improved implementation due to Heiko Bauke. doi:10.1088/0305-4470/29/18/005. All values are available at `http://www-e.uni-magdeburg.de/mertens/research/labs/open.dat`.

[19] B. Bošković, F. Brglez, J. Brest, A GitHub Archive for Solvers and Solutions of the `labs` problem, For updates, see `https://github.com/borkob/git_labs` (January 2016).

[20] S. D. Prestwich, Improved Branch-and-Bound for Low Autocorrelation Binary Sequences, http://arxiv.org/abs/1305.6187.

[21] C. D. Groot, D. Würtz, K. H. Hoffmann, Low autocorrelation binary sequences: exact enumeration and optimization by evolutionary strategies, Optimization 23 (1992) 369–384. doi:10.1080/02331939208843771.

[22] A. Reinholz, Ein paralleler genetischer Algorithmus zur Optimierung der binaren Autokorrelations-Funktion, Master's thesis, Diplom Thesis, Universitaet Bonn (October 1993).

[23] F.-M. Dittes, Optimization on rugged landscape: A new general purpose monte carlo approach, Physical Review Letters 76 (1996) 4651–4655. doi:10.1103/PhysRevLett.76.4651.

[24] B. Militzer, M. Zamparelli, D. Beule, Evolutionary search for low autocorrelated binary sequences, IEEE Transactions on Evolutionary Computation 2 (1) (1998) 34–39. doi:10.1109/4235.728212.

[25] F. Brglez, X. Y. Li, M. F. Stallmann, B. Militzer, Reliable Cost Predictions for Finding Optimal Solutions to LABS Problem: Evolutionary and Alternative Algorithms, in: Fifth Int. Workshop on Frontiers in Evolutionary Algorithms (FEA2003), 2003, `http://militzer.berkeley.edu/papers/2003-FEA-Brglez-posted.pdf`.

[26] F. Brglez, X. Y. Li, M. F. Stallmann, B. Militzer, Evolutionary and Alternative Algorithms: Reliable Cost Predictions for Finding Optimal Solutions to the LABS Problem, `http://militzer.berkeley.edu/papers/2003-InfoSciences-accp-FB.pdf`.

[27] S. D. Prestwich, Exploiting relaxation in local search for LABS, Annals of Operations Research 156 (1) (2007) 129–141.doi:10.1007/s10479-007-0226-9.

[28] S. Halim, R. H. Yap, F. Halim, Engineering stochastic local search for the low autocorrelation binary sequence problem, in: Proceedings of the 14th international conference on Principles and Practice of Constraint Programming, CP '08, Springer-Verlag, Berlin, Heidelberg, 2008, pp. 640–645. doi:10.1007/978-3-540-85958-1_57

[29] P. Borwein, R. Ferguson, J. Knauer, The merit factor problem, in: London Mathematical Society Lecture Note Series, Vol. 352, 2008, pp. 52–70. `http://www.cecm.sfu.ca/personal/pborwein/PAPERS/P218.pdf`.

[30] J. E. Gallardo, C. Cotta, A. J. Fernández, Finding low autocorrelation binary sequences with memetic algorithms, Appl. Soft Comput. 9 (4) (2009) 1252–1262. doi:10.1016/j.asoc.2009.03.005.

[31] M. J. Golay, The merit factor of legendre sequences, IEEE Transactions on Information Theory IT-29 (6) (1983) 934–936. doi:10.1109/TIT.1983.1056744.

[32] J. Jensen, H. Jensen, T. Hoholdt, The merit factor of binary sequences related to difference sets, Information Theory, IEEE Transactions on 37 (3) (1991) 617–626. doi:10.1109/18.79917.

[33] P. Borwein, K.-K. Choi, J. Jedwab, Binary sequences with merit factor greater than 6.34, Information Theory, IEEE Transactions on 50 (12) (2004) 3234–3249. doi:10.1109/TIT.2004.838341.

[34] R. A. Kristiansen, M. G. Parker, Binary sequences with merit factor > 6.3, Information Theory, IEEE Transactions on 50 (12) (2004) 3385–3899. doi:10.1109/TIT.2004.838343.

[35] J. Jedwab, D. J. Katz, K.-U. Schmidt, Advances in the Merit Factor Problem for Binary Sequences, J. Comb. Theory Ser. A 120 (4) (2013) 882–906. doi:10.1016/j.jcta.2013.01.010.

[36] J. Jedwab, D. J. Katz, K.-U. Schmidt, Littlewood polynomials with small L^4 norm, Advances in Mathematics 241 (2013) 127 – 136. doi:10.1016/j.aim.2013.03.015.

[37] J. Baden, Efficient optimization of the merit factor of long binary sequences, Information Theory, IEEE Transactions on 57 (12) (2011) 8084–8094. doi:10.1109/TIT.2011.2164778.

[38] F. Brglez, Of n-dimensional Dice, Combinatorial Optimization, and Reproducible Research: An Introduction, Eletrotehniški Vestnik 78(4) 2011: pp. 181–192, English Edition, `http://ev.fe.uni-lj.si/4-2011/Brglez.pdf` ; An invited talk at 2011-ERK, Portoroz, Slovenia, Sept. 2011 78 (4) (2011) 181–192.

[39] F. Brglez, Self-Avoiding Walks across n-Dimensional Dice and Combinatorial Optimization: An Introduction, Informacije MI-DEM, 44 (1) (2014), pp. 53-68, English Edition `http://www.midem-drustvo.si/journal/` ; also at `http://arxiv.org/abs/1309.7508` ; An invited talk at 2013-MIDEM, Sept. 2013, Kranjska Gora, Slovenia 44 (1) (2014) 53–68.

[40] Self-avoiding walk (2014) [cited 2014].
http://en.wikipedia.org/wiki/Self-avoiding_walk

[41] G. Slade, The self-avoiding walk: A brief survey, in: J. Blath, P. Imkeller, S. Rœlly (Eds.), Surveys in Stochastic Processes, European Mathematical Society, 2011, pp. 181–199.
https://www.math.ubc.ca/~slade/spa_proceedings.pdf.

[42] N. Madras, G. Slade, The Self-Avoiding Walk, Modern Birkhäuser Classics, 2013. doi:10.1007/978-1-4614-6025-1.

[43] N. Clisby, Efficient Implementation of the Pivot Algorithm for Self-avoiding Walks, Journal of Statistical Physics 140 (2010) 349–392. doi:10.1007/s10955-010-9994-8.

[44] F. Brglez, J. Brest, B. Bošković, xBed: An Open Environment for Design and Experiments with Combinatorial Solvers, A preprint available from the authors.

[45] Pranab Kumar Sen, Censoring in Theory and Practice: Statistical Perspectives and Controversies, Institute of Mathematical Statistics, Analysis of Censored Data 27 (1995) 177–192. doi:10.1214/lnms/1215452220.

[46] SLING - Slovenian Initiative for National Grid,
See http://www.sling.si/sling/ for an overview (2014).

[47] I. Olkin, L. J. Gleser, C. Derman, Probability Models and Applications, Macmillan Publishing Co., Inc., 1980.

[48] The R Project for Statistical Computing,
http://www.r-project.org/ (Nov 2015).

[49] A dedicated 'sam cluster' of 22 processors., NCSU High Performance Computing Services. See also http://www.ncsu.edu/itd/hpc/ for an overview (2013).

[50] LABS Problem: 2002 Merit Factor Records posted by Knauer, Now re-posted under https://github.com/borkob/git_labs (2016).

[51] J. Trastoy, M. Malnou, C. U. R. Bernard, N. Bergeal, G. Faini, J. Lesueur, J. Briatico, J. E. Villegas, Freezing and thawing of artificial ice by thermal switching of geometric frustration in magnetic flux lattices, Nat Nano 9 (9) (2014) 710–715. doi:10.1038/nnano.2014.158

[52] F. Brglez, On Stochastic Combinatorial Optimization and Markov Chains: from Walks with Self-Loops to Self-Avoiding Walks, A preprint available from the author.

[53] F. Brglez, B. Bošković, J. Brest, On Asymptotic Complexity of the Optimum Golomb Ruler Problem: From Established Stochastic Methods to Self-Avoiding Walks, A preprint available from the authors.

[54] C. Cotta, . Dotu, A. J. Fernandez, P. V. Hentenryck, A Memetic Approach to Golomb Rulers, in: T. P. Runarsson et al (Ed.), Parallel Problem Solving from Nature, LNCS, Springer, 2007, pp. 252–261. doi:10.1007/11844297_26.

[55] Golomb Rulers Project,
http://www.distributed.net/OGR (2016).

[56] Golomb Ruler Wikipedia,
http://en.wikipedia.org/wiki/Golomb_ruler (2016).

[57] E. R. Tufte, Beautiful Evidence, Graphics Press LLC, 2006.